Genetically silencing CA3 output reveals CA3 transmission is responsible for the bilateral integration of CA1 spatial coding in mice

CA3 出力の遺伝学的抑制により明らかになったマウス CA1 の空間符号化の両側統合における CA3 伝達の重要性

December, 2021

Hefei GUAN

関　鶴菲

Genetically silencing CA3 output reveals CA3 transmission is responsible for the bilateral integration of CA1 spatial coding in mice

CA3 出力の遺伝学的抑制により明らかになったマウス CA1 の空間符号化の両側統合における CA3 伝達の重要性

December, 2021

Waseda University

Graduate School of Advanced Science and Engineering

Department of Life Science and Medical Bioscience

Research on Neurophysiology

Hefei GUAN

関　鶴菲

Acknowledgements

First of all, I would like to thank my PhD supervisor at RIKEN CBS, Dr. Thomas McHugh, who influenced me a lot with his great knowledge of neuroscience. He not only provided a creative research environment, but also taught me how to think independently and do research collaboratively as a neuroscientist. His patient and unconditional supports encouraged me during my PhD, especially when I felt like I should give up with my project. His wisdom and massive reading of literatures always enlightened me and give me new ideas about neuroscience. Secondly, I am also very grateful to my supervisor in Waseda University, Professor Takafumi Inoue, who served as my supervisor since beginning my master degree. He introduced me a broader world of neuroscience during my master course and constantly supported me during my PhD course. He gave me insightful comments for my thesis and project, and I learned in discussion with him.

I thank all the members of CBP at RIKEN CBS, who discussed my research and gave me technical supports. In particular, I would like to thank Dr. Steven Middleton, who is not only the mentor of my research project, but also a great friend of mine in the lab. He showed me how to do experiments, as well as how to read and write code in Matlab to analyze data from the zero level. Without his patient and detailed support, I wouldn't have been able to finish my PhD. I also thank Dr. Takeru Matsuda at RIKEN CBS, who gave me advice on statistical analysis.

Last but not the least, I am grateful for my family, who give me the most support in my life. I thank my mom for her help of taking care of my boy, which allowed me to continue my studies right after giving birth. Also I am thankful to my husband, Zheng Wang, whose love, trust and unconditional support made my PhD come true. His discussion and advice from the perspective of a different field gave me great help for my project. His company witnessed my growth.

Abstract

The spatial code observed in the rodent hippocampus(O'Keefe and Dostrovsky 1971) has been a crucial tool in the dissection of fundamental memory mechanisms(Foster and Wilson 2006, Pfeiffer and Foster 2013, Schiller, Eichenbaum et al. 2015). Previous works have demonstrated that CA3 input plays a critical role in the organization of CA1 population activity, during both learning and periods of consolidation(Nakashiba, Young et al. 2008, Nakashiba, Buhl et al. 2009, Middleton and McHugh 2016, Yamamoto and Tonegawa 2017, Davoudi and Foster 2019). Though this circuit has been well studied, little attention has been paid to the bilateral nature of the CA3 projections to CA1, with their contribution to memory dependent processes poorly understood. Also, it remains unclear if the experience-dependent sequential "replay" of place cells which occurs during sharp-wave ripples (SWRs), population events correlated with memory consolidation(Ego-Stengel and Wilson 2010, Buzsaki 2015), remains intact in the absence of CA3 transmission. A further gap in our understanding of circuit function is if the functional lateralization observed in the human hippocampus(Burgess, Maguire et al. 2002, Maguire and Frith 2003) is present in rodents and what circuitry may underlie it. Previous works in mice, largely focused on hemispheric differences in receptor expression(Kawakami, Shinohara et al. 2003), dendritic morphology, in vitro electrophysiology and behavior, have argued for lateralization(Jordan 2020), primarily attributing to differences in the bilateral CA3 projections to CA1(Shinohara, Hirase et al. 2008, Kohl, Shipton et al. 2011, Shipton, El-Gaby et al. 2014). Further, several in vivo physiological studies, again primarily focused on CA3, have observed some hemispheric differences(Benito, Martín-Vázquez et al. 2016, Villalobos, Maldonado et al. 2017, Song, Wang et al. 2020). However, bilateral recordings of place cell activity in the rat hippocampus consistently found similar and integrated activities in the left and right CA1(Carr, Karlsson et al. 2012, Pfeiffer and Foster 2013). Given the lack of robust direct contralateral connections in CA1, a parsimonious interpretation of these data is that bilaterally projecting CA3 inputs may be crucial for integrating the left and right CA1 during memory, however this has not been directly examined.

Here I investigated the role of CA3 output on memory encoding and reactivation across bilateral CA1, by blocking synaptic transmission at CA3 terminals through the inducible transgenic expression of TeTX. Although the properties of single place cells in CA1 were comparable bilaterally, I found a decrease of ripple synchronization between left and right CA1 after silencing CA3. Further, I observed degradations in replay (the reactivation of previously explored spatial paths) in CA1, consistent with the idea that CA3 bilateral projections coordinate the CA1 activity across hemispheres. In summary, my results demonstrate that CA3 input to CA1 organizes the activity not only within single hemispheres but also bilaterally across both CA1s, with its absence memory encoding and retrieval are impaired.

Table of Contents

Acknowledgements 3

Abstract 4

Table of Contents 6

List of Figures 10

1 Introduction 12

1.1 Hippocampus and memory 12

1.1.1 Hippocampus and episodic memory 12

1.1.2 Hippocampus and spatial memory 14

1.2 Hippocampal formation and the hippocampal circuits 19

1.2.1 Circuits of the hippocampal formation 19

1.2.2 CA3-CA1 circuit 21

1.3 Hippocampal lateralization 23

1.3.1 Lateralization in the human brain 23

1.3.2 Lateralization in the rodent hippocampus 24

1.4 Sharp wave ripples 25

1.4.1 Properties of SWRs 26

1.4.2 Origin of SWRs 28

1.4.3 Function of SWRs in memory processes 29

1.5 Cell assemblies 30

1.6 Replay 32
1.6.1 Replay events 32
1.6.2 Bayesian replay analysis 34
1.6.3 Per cell contribution for each replay event 35
1.7 CA3-TeTX mice 36
1.8 Previous research and unanswered questions 39
1.8.1 Previous research using CA3-TeTX mice 39
1.8.2 Silencing bilateral CA3 input by optogenetic tools in mice resulted in a dramatic decrease of SWRs and replay in unilateral CA1 41
1.8.3 Silencing bilateral CA3 input by optogenetics tools in rat impaired SWRs and quality of replay in bilateral CA1. 41
2 Materials and Methods 44
2.1 Subjects 44
2.2 Surgery and recording preparation 44
2.3 Recording protocol 47
2.4 Place cell analyses 48
2.4.1 Cell cluster and pyramidal cell classification 48
2.4.2 Definition of place cells properties 49
2.4.3 Spatial Information 49
2.5 Cell assembly analyses 50
2.5.1 Assembly pattern identification 50

2.5.2 Unilateral and bilateral assembly detection 51
2.5.3 Shuffling of member neurons in each cell assembly 51
2.5.4 Tracking expression of assembly patterns over time 51
2.6 Ripple detection 52
2.7 Ripple synchronization 52
2.8 Bayesian replay analyses 53
2.9 Per cell contribution (PCC) analyses 55
2.10 Statistics 55
2.10.1 Wilcoxon rank sum test 56
3 Results 57
3.1 Pyramidal cell properties remain similar across bilateral CA1 after silencing CA3. 57
3.2 Decrease in bilateral CA1 cell assemblies following the silencing of CA3 input. 60
3.3 SWRs and associated assembly reactivation are lateralized in CA3-TeTX mice. 63
3.4 CA3 input is required for replay sequences across bilateral CA1. 67
4 Discussion 71
4.1 Overall discussion 71
4.2 The importance of bilateral CA1 recording in mice. 72
4.3 Cell assemblies and replay 73
4.3.1 Increased strength of cell assemblies during SWRs following CA3 inhibition 73
4.3.2 Preserved replay 74
4.3.3 Cell assemblies vs. Replay 75

4.4 Behavioral impact related to increased lateralization by silencing CA3 76

4.5 Advantages and limitation of this study 77

4.5.1 Advantages and limitation of CA3-TeTX transgenic mice 77

4.5.2 Limitation of using only male mice in this study 78

4.6 Future directions 78

4.6.1 Dissociation of CA3-ipsilateral CA1 and CA3-contralteral CA1 projections 78

4.6.2 Functional dissociation of left and right CA3. 79

4.6.3 Effect of simultaneously silencing CA3 and CA2 on neural activity in bilateral CA1 .. 80

5 Conclusion 81

6 Reference List 83

List of Figures

Figure 1.1 Theta phase precession 18

Figure 1.2 Hippocampus consists of DG, CA1, CA2 and CA3. 20

Figure 1.3 CA3 pyramidal neurons project to both ipsi- and contralateral CA1..... 23

Figure 1.4 Examples of filtered ripple (a), sharp wave (b), and SWRs (c). 27

Figure 1.5 Single pyramidal cells fire during SWRs. 28

Figure 1.6 Cell assembly 32

Figure 1.7 Replay event..... 34

Figure 1.8 Per Cell Contribution (PCC) calculation..... 36

Figure 1.9 CA3-TeTX mice is a triple transgenic mouse line..... 37

Figure 1.10 Tetanus Toxin blocks neurotransmitter release. 38

Figure 1.11 Expression of VAMP2 in the slices of CA3-TeTX mutant and control mice. 39

Figure 2.1 Micro-drive array. 45

Figure 2.2 Different views of an example micro-drive prior to implantation surgery. 45

Figure 2.3 An example of implantation surgery. 46

Figure 2.4 Histology shows tetrode locations in left and right hippocampal CA1..... 46

Figure 2.5 2D views showing clustered neurons of two different tetrodes. 48

Figure 2.6 Calculation of the cross-correlation of SWR events from bilateral CA1. 52

Figure 3.1 Pyramidal cell properties remain similar across bilateral CA1 after silencing CA3. 60

Figure 3.2 Silencing CA3 input decrease bilateral CA1 cell assemblies, but assembly size and participation keep similar. 62

Figure 3.3 Cell assemblies were lateralized by silencing CA3 input. 63

Figure 3.4 SWRs properties across genotypes and hemispheres, and gamma oscillations across hemispheres. 65

Figure 3.5 CA3 input is required for bilateral coordination of assembly reactivation. 67

Figure 3.6 CA3 input is required for bilateral replay sequences in CA1. 68

Figure 3.7 CA3 input is required for bilateral coordination replay sequences in CA1 70

1 Introduction

The spatial code observed in the rodent hippocampus (O'Keefe and Dostrovsky 1971) has been a crucial tool in the dissection of fundamental memory mechanisms(Foster and Wilson 2006, Pfeiffer and Foster 2013, Schiller, Eichenbaum et al. 2015). Previous works have demonstrated that CA3 input plays a critical role in the organization of CA1 population activity, during both learning and consolidation (Nakashiba, Young et al. 2008, Nakashiba, Buhl et al. 2009, Middleton and McHugh 2016, Yamamoto and Tonegawa 2017, Davoudi and Foster 2019). However, it remains unclear if the experience-dependent sequential "replay" of place cells which occur during sharp-wave ripples (SWRs), population events correlated with memory consolidation(Ego-Stengel and Wilson 2010, Buzsaki 2015), remains intact in the absence of CA3 transmission. A further gap in our understanding of circuit function is if the functional lateralization observed in the human hippocampus (Burgess, Maguire et al. 2002, Maguire and Frith 2003) is present in rodents and what circuitry may underlie it. Previous work in mice, largely focused on hemispheric differences in receptor expression(Kawakami, Shinohara et al. 2003), dendritic morphology, in vitro electrophysiological and behavior, has argued for lateralization(Jordan 2020), primarily attributed to differences in the bilateral CA3 projections to CA1(Shinohara, Hirase et al. 2008, Kohl, Shipton et al. 2011, Shipton, El-Gaby et al. 2014). However, bilateral recordings of place cell activity in the rat hippocampus consistently finds similar and integrated activity in the left and right CA1(Carr, Karlsson et al. 2012, Pfeiffer and Foster 2013). Given the lack of robust direct contralateral connections in CA1, a parsimonious interpretation of these data is that bilaterally projecting CA3 inputs may be crucial for integrating the left and right CA1 during memory, however this has not been directly examined.

1.1 Hippocampus and memory

1.1.1 Hippocampus and episodic memory

The hippocampus is one of the most widely studied area of brain, and in humans it has been shown to be crucial for episodic memory (Andersen, Morris et al. 2006). The term episodic memory was first coined

by Endel Tulving in 1972 to describe humans' ability to remember the timing, content and location of events they experience (Tulving 1983). Although central to our identities, the capacity for long-term episodic memory appears late in human development, around the age of four years old when the hippocampus fully matures (Scarf, Gross et al. 2013), and remains susceptible to diseases across our lives, as it is one of the first types of memory to disappear in humans suffering from Alzheimer's Disease(Andersen, Morris et al. 2006).

The study of the role of the human hippocampus in memory began with one of the most well-known patients in neuroscience, Henry Molaison (H.M). When Henry was in his late 20's surgeons removed one section from each side of his bilateral medial temporal lobe (MTL) in order to relieve severe epilepsy. After the surgery his seizures abated, however he suffered from a persistent anterograde impairment of episodic memory and a time-dependent retrograde amnesia, which spared older memories, such as those from his childhood. Moreover, his technical and motor skills remained intact. Together with other patients who experienced MTL damage of differing degrees and locations, Henry's impairments confirmed that the hippocampus and the parahippocampal structures are critical for the acquisition of both short-term and long-term memory of new events, however the persistence of older episodic memories indicates that while the MTL is necessary for the encoding and recent storage of these memories, it may not be absolutely required for their permanent storage (Scoville and Milner 1957).

While there is consensus that interactions between the hippocampus and cortex following memory encoding is required for long-term storage, a process termed systems consolidation(Rothschild, Eban et al. 2017), the precise contribution of the hippocampus to the recall of remote episodic memories still remains disputed, with some studies claiming a continued role of the structure even for distant memories (Steinvorth, Levine et al. 2005). This theory claims that although remote episodic memories are already stored stably in cortex following transfer from the hippocampus, the retrieval of the stored episodic memory remains dependent on the connectivity with hippocampus. Although this theory based largely on rodent experiments seems to be in conflict with the case of H.M., who's remote memories preceding damage to the MTL

remained intact, it is possible that H.M.'s remote memory lacked the full details of episodic memory, similar to the more generalized memories spared in rodents following hippocampal damage.

1.1.2 Hippocampus and spatial memory

While episodic memory has been primarily studied in humans, research on the rodent hippocampus has focused on its role in spatial memory. This is explained by the seminal discovery of the existence of "place cells" in the rodent hippocampus by O'Keefe and Dostrovsky (O'Keefe and Dostrovsky 1971, O'Keefe and Nadel 1978), as well as behavioral studies conducted around the same time that found that rats with damage in the hippocampus showed a deficit in spatial memory (Morris, Garrud et al. 1982).

The hippocampus is different from other cortical areas in that it is mainly responsible for allocentric spatial memory, while other areas, such as parietal cortex, are more responsible for egocentric spatial memory (O'Keefe and Nadel 1978, Morris, Garrud et al. 1982, Eichenbaum, Stewart et al. 1990). In the human, tasks that engage allocentric spatial memory do trigger activity in the hippocampus, however it appears in a more lateralized fashion, primarily in the right hippocampus. In contrast, the left hippocampus is more involved in episodic memory, which I will explain in detail in the subsequent section on lateralization.

1.1.2.1 Place cells and place fields

In the initial experiments by O'Keefe and Dostrovsky hippocampal neuronal activity was recorded via microelectrodes while rats explored platforms or simple mazes. They found that some cells in dorsal CA1 only fired when animal passed through a particular location, which they termed place fields, and the cells were named as place cells. This discovery led to the proposal of the cognitive map theory of hippocampal memory (O'Keefe and Nadel 1978), which suggested that the hippocampal representation of space and context, along with its sensitivity to the context of the environment during navigation could provide a framework for the anchoring of memories.

The initial discovery of place cells in the hippocampus launched an entire field of study focused on understanding their mnemonic and physiological properties. One of the initial lines of inquiry was focused on understanding the sensory inputs that drive the space specific responses of the neurons. For example, early experiments demonstrated that when a platform is rotated in relation to the room the place fields would also rotate in respect to the dominant visual cue (O'Keefe 1976). A later example of the allocentric nature of the representation of space in the hippocampus and its links to memory was the discovery of replay, which is the sequential firing of place cells during sharp-wave ripples (SWRs), population events correlated with memory consolidation (Ego-Stengel and Wilson 2010, Buzsaki 2015), which reflects the order of their activity during exploration (Pfeiffer and Foster 2013). Replay is thought to be an example of allocentric spatial representation, as it can reflect the spatial representation of environment outside times of active exploration (Danjo 2020). In addition, the phenomenon of preplay, which occurs before exploring novel environments, suggested that the hippocampus is able to allocate preexisting ensembles to encode spatial information of the environment (Dragoi and Tonegawa 2011). In research published by Danjo et al., which recorded from rats performing a task in which they were required to observe the location of another animal, the place cells in CA1 of the recorded animals were affected not only by their own locations, but also by the locations of their counterparts. This further suggests that the place cells in hippocampus preferentially represent allocentric spatial information (Danjo, Toyoizumi et al. 2018).

Visual input is not absolutely required for place responses, as place cell activity persists even when the rooms lights are turned off.(O'Keefe 1976), suggesting that the space-specific firing is not maintained by a single sensory stimulus. Rather, what is thought to drive place cell firing is a more complex combination of stimuli, or perhaps by the more abstract conjunctive term such as location; moreover, the tuning of place cells can be impacted by path integration, internal information about one's own motion through space, which is independent of external spatial cues (Etienne and Jeffery 2004). Consistent with this, when animals are placed in a cylindrical apparatus, of which the floor and wall can be rotated independently, inputs of both visual and locomotor cues were shown to have influence on place fields (Sharp, Blair et al. 1995). It

has also been shown that the firing properties of place cells can be altered when only locomotor cues were used during exploration (Etienne and Jeffery 2004).

The locations where place cells fire when an animal explores are relatively stable in a familiar environment, suggesting that the hippocampus forms a stable long-term spatial memory of that context (Thompson and Best 1990). However, more recent experiments using Ca^{2+} imaging to track the place fields of pyramidal cells in CA1 over weeks have revealed that a significant fraction of place cells tend to fire in a different location over time, with a decreased overlap in place coding and only 15-25% of cells displaying stable place fields across the timescale of a month (Ziv, Burns et al. 2013). When a rodent is put into a clearly different context the representation of place cells changes, with a new, uncorrelated firing patterns of place cells. Experimentally, it has been shown that a place cell map recorded in hippocampal CA3 can represent eleven totally different maps for eleven different rooms, suggesting the spatial representation of distinct contexts in CA3 are highly independent (Alme, Miao et al. 2014). This phenomenon of unique maps for distinct contexts is called remapping (Bostock, Muller et al. 1991). In the context of the cognitive map theory, remapping may act as a mechanism for differentiating memories, as it has been shown by McHugh et al. that the remapping of place cells in CA3 was disrupted in mutant mice lacking NMDA receptors in DG, mice that had behavioral deficits in distinguishing similar contexts (McHugh, Jones et al. 2007).

1.1.2.2 Spatial information of place cells

Much of the more recent work in the place cell field has been focused on quantitative measures of the underlying physiology of neurons and changes that occur following manipulation of specific parts of the circuitry. The simplest variables to quantify include average and peak firing rates, size of place fields, and the spatial information of neurons. For example, in the paper published by Davoudi et al., the authors concluded that inhibiting CA3 pyramidal cell axons in CA1 reduced the place field responses in CA1, noting significant decreases in field peak rate, field size, and the location of the field's center of mass over time; however the spatial information per spike increased (Davoudi and Foster 2019). The intuitive meaning

of most of these properties can be easily recognized, perhaps with the exception of spatial information, which is thought to be one of the most important properties of a place field. Spatial information mathematically captures how well the firing of a neuron predicts the location of animal, representing the amount (bits) of information represented as a function of time or per spike of a place cell as an animal runs through the environment. For example, place cells with smaller spatial information typically show more diffused place fields, while high spatial information neurons have compact and cohesive fields. Spatial information can be applied to compare the quality of place cells under different conditions. For example, the spatial information of cells recorded when an animal is in an environment with proximal cues is much higher than that in the same environment with only distal cues. This results suggested that stable proximal visual cues are important for the information content of place cells (Skaggs, McNaughton et al. 1993). If an animal is exposed to the same environment multiple times the average spatial information of the active place cells increases acrossvisits, suggesting that the spatial information is also dependent on experience (Cacucci, Wills et al. 2007). Consistent with this, spatial information of place cells in mice lacking NMDA receptor-dependent synaptic plasticity remains relatively low, even after the mutant animals have been familiarized with the environment (McHugh, Blum et al. 1996).

1.1.2.3 Firing pattern of place cells during the theta cycle

During locomotion the hippocampal local field potential is dominated by several prominent rhythms that can be classified by their frequency. Among them, the most dominant are oscillations in the frequency band of 7-12 Hz, classified as theta waves. In rats, theta occurrence is strongly correlated with animal movement, including walking, running, rearing, swimming, jumping, exploring, etc. Previous studies have established that, on average, there is a correlation between the phase of the theta oscillation and the probability of spiking of hippocampal place cells, with the preferred phase corresponding roughly to the trough of the oscillation (Skaggs, McNaughton et al. 1996). However, spikes are not confined to a single section of the oscillation and when researchers took a more careful look at the relative phase of spikes across a single place field they uncovered a more precise manner of temporal coding (O'Keefe and Recce

1993). Specially, as a rodent moves through a field, the place cells' theta phase preference changes in a systematic way, with the first spike of place cells occurring at a relatively late phase of theta and subsequent spikes shifting to an earlier phase in the next theta cycle. This precession across the phase continues within the whole field, so when the animal leaves the field, the phase shift has moved across a whole cycle of the theta wave (O'Keefe and Recce 1993). This phenomenon, termed theta phase precession, is shown in the cartoon model in Figure 1.1.

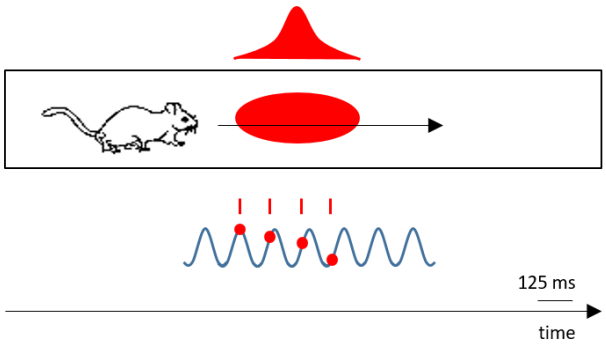

Figure 1.1 Theta phase precession

When the relationship of the spikes of many simultaneously recorded place cells within a theta cycle is examined a more striking pattern across the population emerges: with the relative temporal order of the place cells firing spikes within a single theta cycle forming a compressed sequences reflecting the order of their average firing fields on the track; a process termed theta sequences (Dragoi and Buzsaki 2006, Foster and Wilson 2007). Different from replay sequences, which re-express the behavioral order of cell spiking during SWRs in the post-exploration session (will be introduced in the section 1.6, Replay), theta sequences occur during exploration and may be important for synaptic strengthening during memory encoding. It has also been suggested that a function of theta sequences is to retrieve information, as they reflect spatial information ahead of the animal during exploration (Buzsaki 2005).

1.1.2.4 Social-place cells

One recent interesting study about place cells worth mentioning here described social-place cells in the dorsal CA1 of the bat hippocampus, which reflected the location, in allocentric coordinates of other animals (Omer, Maimon et al. 2018). In this study, the authors showed that half of the cells represented both the bat's own positions as well as the other animals' positions at the same time, which they termed "social place-cells". The feature of these social place cells suggested that the spatial coding of other animal locations is not related to any specific sensory input. They also embodied the cognitive representation of the environment, overlapping with the traditional place cell concept. At the same time, data consistent with this was reported from rat hippocampus; Danjo et al. showed that when other conspecific's behavior was required for a rat to retrieve reward in a T-maze task, the place cells of the recorded rats represented the locations of both self and other conspecific, information important for social behavior (Danjo, Toyoizumi et al. 2018).

1.2 Hippocampal formation and the hippocampal circuits

1.2.1 Circuits of the hippocampal formation

The hippocampus is a part of the larger hippocampal formation, which consists of the hippocampus (proper), subiculum, presubiculum, parasubiculum and entorhinal cortex (EC). The EC can be further divided into the lateral entorhinal cortex (LEC) and medial entorhinal cortex (MEC), while the hippocampus consists of four distinct subfields, CA1, CA2, CA3 and the dentate gyrus (DG) (Figure 1.2) (Hartley, Lever et al. 2014). Within the hippocampal formation, excitatory neurons form unique, largely unidirectional connections with each other. In the EC, neurons in layer II send projection to DG, CA3 and CA2, while neurons in layer III send projection to CA1 and subiculum. In the DG the primary excitatory neurons are granule cells, which send projection to CA3 and to some neurons in CA2. In CA3, pyramidal cells send projection to the stratum radiatum (SR) of CA1 and CA2, as well as recurrent projections within CA3, both ipsi- and contralaterally. In CA2, pyramidal cells mainly project to stratum oriens (SO) of CA1,

but also possess CA2 targeting recurrent connections and projections back into CA3 (Middleton and McHugh 2019). In CA1, pyramidal cells project primarily to subiculum, although direct projections back to deeper layers of the EC have been identified. Finally, the subiculum also sends projection back to the deep layer of EC, as well as other cortical and subcortical targets. Figure 1.2 highlights the projections that CA1 receives from other hippocampal areas.

Within the circuit the pyramidal cell in the CA regions is considered the major type of excitatory neuron in hippocampus and plays the key role in receiving input and sending output from and to other areas of the brain. A typical CA1 pyramidal neuron consists of three parts: the cell body, with the shape of upside down pyramid; a longer dendrite extending towards the hippocampal fissure, termed the apical dendrite; and a shorter clustered dendrite in SO, called the basal dendrite (Cembrowski and Spruston 2019).

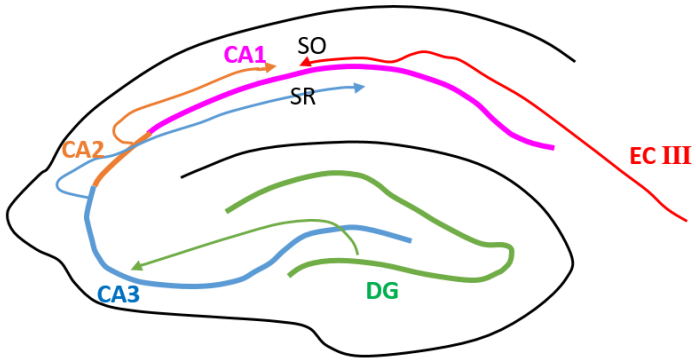

Figure 1.2 Hippocampus consists of DG, CA1, CA2 and CA3.

Research has been focused on how the complex connections within the hippocampal formation are related to its physiology and animal behavior. Disruptions of the circuit, both within the hippocampus proper and projections from other cortical area connected to hippocampus, have been shown to lead to memory impairments, helping us to better understand the mechanisms of memory formation, consolidation and recall. For example, it has been shown that CA3 transmission is required for memory encoding in novel environment (Nakashiba, Young et al. 2008), as well as the consolidation of fear memory in familiar contexts (Nakashiba, Buhl et al. 2009). It has also been shown that silencing CA2 output led to a deficit in

social memory in rodents, while spatial and contextual memory remained intact (Hitti and Siegelbaum 2014). In addition, silencing the input from layer III of MEC reduced not only SWRs in CA1, but also the replay events that are thought to be important for memory consolidation and retrieval (Yamamoto and Tonegawa 2017).

It has long been known that long-term potentiation (LTP) in CA1 is blocked by antagonists of the NMDA receptor (Collingridge, Kehl et al. 1983). By using mice with a CA1 pyramidal cell-specific NMDA receptor gene knockout it was shown that the loss of LTP resulted in place cells with lower spatial specificity, as well as deficits in the pair-wise coordination of spiking of overlapping place fields (McHugh, Blum et al. 1996). Furthermore, these transgenic mice also showed a disruption of spatial memory acquisition, which suggested that the synaptic plasticity in CA1 is necessary for the acquisition of spatial memory (Tsien, Huerta et al. 1996). Finally, in mice with the same NMDA receptor gene knockout in DG granule cells, contextual memory was normal, however the ability of the animals to distinguish between similar contexts was impaired, suggesting that DG synaptic plasticity plays an important role in pattern separation and/or contextual discrimination (McHugh, Jones et al. 2007). It has been suggested that this may be mediated by the shaping of CA3 encoding, as CA3 mainly receives input from DG granule cells in addition to the EC (McHugh, Jones et al. 2007).

1.2.2 CA3-CA1 circuit

In this thesis I mainly focus on the circuits among bilateral CA1 and CA3. The bilateral inputs from CA3 are the predominant excitatory drive to CA1, thus understanding their function is crucial for elucidating mechanism of hippocampal memory and physiology.

1.2.2.1 Recurrent network within CA3

As mentioned above, a major excitatory input to CA3 pyramidal cells are recurrent collaterals originating from CA3 of both hemispheres. The pyramidal neurons of CA3 target both themselves and interneurons through these recurrent collaterals, known as associational connections. The CA3 pyramidal

neurons also project to the contralateral CA3 through the commissural fiber, which exist in SO and SR. The density of this projection within CA3 is not symmetric along the transverse and longitudinal axes. For example, neurons in the ventral CA3 project more to the proximal CA3, while neurons in dorsal CA3 project more to the distal CA3 (Ishizuka, Weber et al. 1990). It has been suggested that this recurrent network in CA3 is important for the initial formation of one-trial memory (McHugh and Tonegawa 2009), for pattern completion computations (Nakazawa, Quirk et al. 2002) as well as for the generation of gamma oscillation within the hippocampus (Csicsvari, Jamieson et al. 2003).

1.2.2.2 CA3-ipsilateral CA1 and CA3-contralateral CA1 projections

In addition to the recurrent projection within CA3, CA3 also projects to pyramidal cells and interneurons in the ipsilateral CA1 through the Shaffer collaterals, named after Károly Schaffer who described the 'collateral fiber system' between CA3 and CA1 (Szirmai, Buzsáki et al. 2012). These projections from CA3 mainly target dendrites in the SR and SO of CA1, which are located above (further from cortex) and below (closer to cortex) the pyramidal layer, respectively. CA3 also projects to both dorsal and ventral CA1, and the projections along the longitudinal axis in CA1 cover longer areas than those by the recurrent network of CA3 itself. Moreover, there are patterns of connectivity across the proximal/distal axis of the subfields, with proximal CA3 projecting to distal CA1, and distal CA3 projecting to proximal CA1.

CA3 neurons also target neurons in contralateral CA1 through the commissural fibers (Figure 1.3), although the detailed topography of these circuits has not been investigated as thoroughly as for the ipsilateral connections (Witter 2007). It has been widely thought that the synaptic features are quite similar between ipsilateral CA3-CA1 and contralateral CA3-CA1 connections, with the pyramidal neurons in CA3 sending excitatory projections to both pyramidal neurons and interneurons in CA1. However, recent work has shown that there are substantial differences in the balance of CA3 projections to SO and SR of CA1 between the ipsi- and contralateral pathways. In the SO of anterior CA1 there are more contralateral projections than ipsilateral ones from CA3. However, in CA1 SR, there are more ipsilateral projections than

contralateral ones from CA3 (Shinohara, Hosoya et al. 2012). In addition to the anatomical studies on ipsi- and contralateral CA3-CA1 connections, a study which mapped CA1 responses by stimulation of ipsi- and contralateral CA3 axons in vivo suggested that the laterality of functional connectivity is in accordance with the anatomical results in rat (Finnerty and Jefferys 1993).

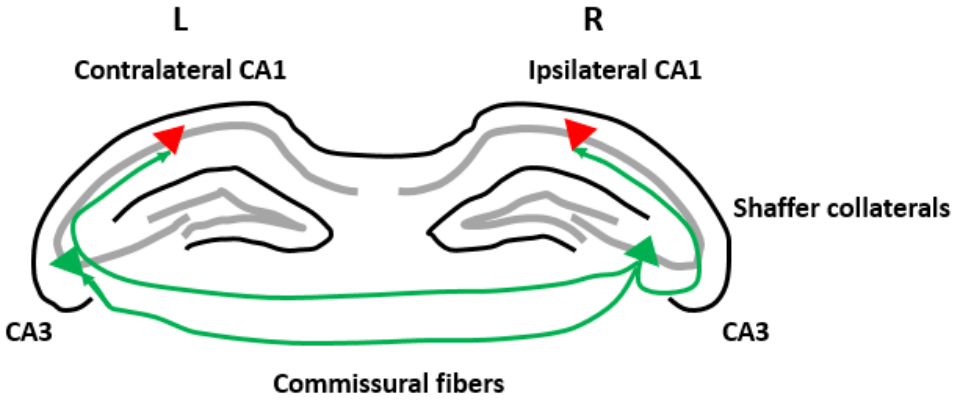

Figure 1.3 CA3 pyramidal neurons project to both ipsi- and contralateral CA1.

1.3 Hippocampal lateralization

1.3.1 Lateralization in the human brain

It has been shown that there are differences in morphology and function between the left and right sides of the central nervous system in several species, but particularly in human beings. This left-right asymmetry of neural substrates or processes, which influence circuit physiology, cognition and behavior, is termed lateralization (Concha, Bianco et al. 2012). In humans, it has been repeatedly shown that the left and right sides of brain are related to different functions, and interpret the same experience in different ways in a given environment (Corballis 2012). It has also been broadly thought that human hippocampus has lateralization of functions related to memory, in which the right hippocampus is more responsible for spatial memory. Conversely, the left hippocampus is more responsible for episodic memory (Burgess, Maguire et al. 2002). However, such lateralization of neural systems, especially in the hippocampus, is diverse across species. In previous research using rodents, the lateralization of hippocampus has been largely ignored, as

it was widely believed that there is stronger bilateral connections between left and right hippocampi in rodents compared to humans which may decrease any functional lateralization.

1.3.2 Lateralization in the rodent hippocampus

Although the lateralization of rodent hippocampus has been largely ignored in previous research, there are several publications focused on its functional and anatomical lateralization, including differences in synaptic plasticity as measured by in vitro electrophysiology. The study by Kawakami et al. is among the earliest research examining lateralization at the microscopic level, in which they reported asymmetrical expressions of Ɛ2 subunits of NMDA receptor in postsynaptic densities between left and right CA1: the expression of Ɛ2 was more distributed in left SR than right, while it was more in right SO than left (Kawakami, Shinohara et al. 2003). They also found an asymmetry of electrophysiological responses mediated by NMDA receptors in hippocampal slices. Consistent with this study, it was shown that there is lateralization of pyramidal cell synapses in CA1, according to the origin of the axons in CA3 (Shinohara, Hirase et al. 2008). The synapses in CA1 that receive input from right CA3 were bigger, with larger post synaptic densities and higher expression of GluR1 than those receiving input from left CA3. However, the lateralized expression of NR2B displayed an opposite pattern; lower expression in the synapses receiving input from right CA3 than those from left CA3.

There were also other electrophysiological studies showing asymmetry in the rodent hippocampal slice. Synaptic terminals of left and right CA3 pyramidal cells in mouse hippocampal slices were stimulated by means of optogenetic tools. It was found that the left CA3 input evoked stronger long-term potentiation at CA1 synapses than right CA3 input did. (Kohl, Shipton et al. 2011). While these studies showed the hemispherical differences in the CA3-CA1 pyramidal cell projection, lateralization of memory processing was not mentioned. Shipton et al. applied optogenetics to acutely silence CA3 pyramidal cells in either the left or right side of mouse hippocampus in vivo while testing memory (Shipton, El-Gaby et al. 2014). It was shown that while there were no differences in short term memory when blocking left or right CA3 input, only the blockade of left CA3 impaired the long-term spatial memory. Consistent with this study, El-

Gaby silenced the CA3- CA1 projections in behaving mice using optogenetics and showed that left CA3 input to CA1 is necessary for the performance of the Y-maze reference memory task, but right CA3 input was dispensable (El-Gaby, Zhang et al. 2016). However, in behavioral tests using the Barnes maze it was suggested that right hippocampus is more important for spatial memory, while no lateralization in non-spatial memory in rodent hippocampus was found (Shinohara, Hosoya et al. 2012).

With the development of novel techniques which allow in vivo recording while rodents are freely moving along with manipulation of the CA3-CA1 circuit more specifically and acutely, experiments were conducted to address the circuit mechanisms of the hippocampal lateralization. Lateralization of gamma oscillations were investigated, as they were thought to be important for cognition and memory. It was found that gamma oscillations were enhanced in CA1 of rats that experienced an enriched environment. In addition, the magnitude of gamma-amplitude enhancement was greater in right hippocampal CA1, and interhemispheric gamma oscillation synchronization was larger in rats reared in an enriched environment compared to those reared in an isolated condition, suggesting that experiencing an enriched environment leads to an asymmetry between left and right hippocampus (Shinohara, Hosoya et al. 2013).

Conclusions of the previous research on rodent lateralization are not consistent, especially across different behavior tasks. The relatively small number of these studies, together with the lack of approaches which permit observation of in vivo neuronal activity from the bilateral hippocampi in the intact brain while an animal is exploring in different environments, have left a gap in our understanding. Thus, research using in vivo electrophysiological recording from bilateral hippocampi is necessary for a better understanding the lateralization of hippocampal circuit in rodent.

1.4 Sharp wave ripples

In vivo electrophysiological recording in the rodent hippocampus allows the monitoring of two types of physiological signals, single cell spiking and local field potential (LFP), the summed extracellular signals

from the population of neurons around the recording electrode. In hippocampal research the primary focus is on four distinct frequency oscillations: the theta (6-12 Hz), beta (12-30 Hz), gamma (30-100 Hz) and ripple (120-200 Hz) band oscillations. These four different oscillations are related to different behaviors and/or activity states and have been suggested to be involved in different mechanisms and periods of memory processing. Most of the early place cell research focused on the temporal coding of cell ensembles during animal motion, during which theta, beta and gamma oscillations mainly occur. For example, the theta waves occur most prominently during movement, such as exploration, walking, swimming, running and so on (Vanderwolf 1969). Place cell spiking has a specific temporal relationship with the theta oscillations, such that spikes tend to fire at progressively earlier phase of each theta cycle as the animal moves through a given place field, a phenomenon termed theta phase precession (O'Keefe and Recce 1993). Moreover, simultaneously recorded place cells fire in a sequence within each theta cycle, with the temporal order of the sequence reflecting the relative order of the place cells as the animal traverses the track. This sequential firing of cells during theta has been termed "theta sequences". The theta sequence represents the sequence of cell activities in a temporally compressed way within the relatively short time window (~125 msec) of a theta cycle, a process suggested to contribute to plasticity during memory encoding. In addition, other work has suggested that theta sequences may also be a mechanism of memory retrieval (Zielinski, Tang et al. 2020).

1.4.1 Properties of SWRs

In contrast to the relatively slow theta oscillation, during rest and slow-wave sleep the hippocampal LFP is dominated by the sporadic occurrence of a large amplitude high-frequency oscillation, between 120 Hz and 200 Hz. This high-frequency oscillation during immobility is called a ripple and is most prominent within the pyramidal layers of CA1 (Figure 1.4a).

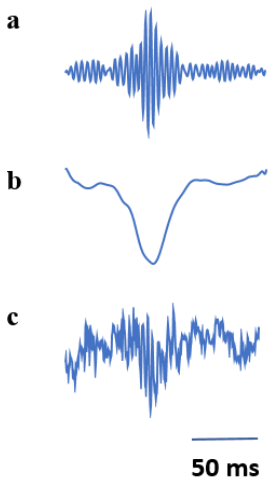

Figure 1.4 Examples of filtered ripple (a), sharp wave (b), and SWRs (c).

Sharp waves, which are found in SR of CA1, typically co-occur with the ripple event and reflect the depolarization of pyramidal cell dendrites receiving input from CA3 pyramidal cells via the Shaffer Collaterals (Figure 1.4b). The sharp wave couples with ripples and forms the sharp wave ripple (SWR) complex (Figure 1.4c; (O'Keefe and Nadel 1978, Buzsáki, Horváth et al. 1992).

During SWRs, single pyramidal cells fire single action potentials, as well as spike bursts (Figure 1.5). Across the population of simultaneously recorded neurons the largest increase in activity is seen during SWRs and within the event, the spikes show strong phase modulation, preferentially occurring during periods of low inhibition at the trough of each ripple wavelet (Buzsaki 2015) (Figure 1.5).

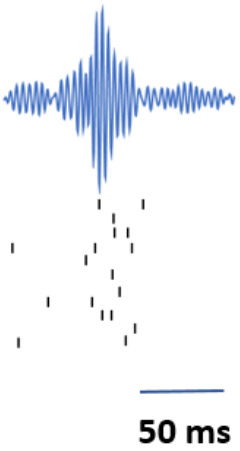

Figure 1.5 Single pyramidal cells fire during SWRs.

Traces filtered for ripple frequency (top), and multiunit activity during SWRs (below).

SWRs have many remarkable features in addition to the ones mentioned above. Neurons that fire during SWRs are activated in a sequential manner, with the firing order in SWRs during post-exploration rest sessions reflecting the firing order of the place cells during exploration (Wilson and McNaughton 1994, Skaggs and McNaughton 1996, Nadasdy, Hirase et al. 1999, Lee and Wilson 2002). As a result, SWRs have been suggested to be a mechanism underlying learning and memory, particularly involved in memory consolidation (Girardeau, Benchenane et al. 2009, Ego-Stengel and Wilson 2010). According to a popular two-step memory consolidation model, the neocortex first supplies novel information to the hippocampus during learning, which leads to a transient change of synaptic organization within its circuits, and then the changed information in hippocampus is transferred to the neocortical circuits during memory consolidation, which was thought to be mediated by SWRs (Buzsaki 1989). Experiments linking SWRs to memory consolidation are discussed below.

1.4.2 Origin of SWRs

It has been suggested that CA3 input triggered by a population activation of pyramidal neurons in CA3 is critical for the generation of SWRs in CA1 (Buzsaki 1986). Consistent with this, it has been shown that

the peak of SWRs in CA3 occurs 4.46 ms earlier than in CA1 on average (Sullivan, Csicsvari et al. 2011). In addition, in the dentate gyrus, the peak of SWRs-related activity occurs 5.34 ms later than in CA1 on average, again supporting the idea that CA3 is the origin of SWRs. In addition to the recorded data, the existence of a recurrent excitatory network within CA3 also bolsters this hypothesis, as it is reasonable to conclude that the recurrent excitation induces a high frequency synchronized oscillation. As the CA3 sends dense projections to CA1, the highly synchronized oscillations are thought to arise from the CA3 activity and spread to CA1 through axonal projections.

In addition to CA3, Oliva et al. have recently suggested that SWRs might also be generated in CA2, as the activation of cells in CA2 can be observed earlier than that in CA1 and CA3 in a subset of SWRs. Detailed recording approaches have localized this activity to cells in the deep layer of CA2 which increase firing before the occurrence of some SWRs; in these events the average peak of ripples in CA2 appeared earlier than that in CA3 (Oliva, Fernandez-Ruiz et al. 2016). In addition, recent work from Imbrosci et al. showed the the subiculum can also serve as a secondary generator of SWRs, which propagate to both the EC and hippocampus, with the authors providing both in vitro and in vivo evidence (Imbrosci, Nitzan et al. 2021). These results suggest that SWRs may have multiple origins, including the subiculum, CA2 and CA3, all of which may contribute to the consolidation of memory in hippocampus.

1.4.3 Function of SWRs in memory processes

Several lines of experimental evidence directly support the idea that SWRs are crucial for memory. It has been shown that the reactivation of cells during SWRs can facilitate the consolidation of memory. When neural activity during SWR events was disrupted by stimulation of hippocampal afferents during a post learning rest session, spatial learning in a hippocampus-dependent maze task was significantly poorer (Ego-Stengel and Wilson 2010). Moreover, it also has been shown that the disruption of SWRs and related neural activities through the stimulation of the ventral hippocampal commissural fibers resulted in a deficit of performance in an eight-arm radial maze task (Girardeau, Benchenane et al. 2009).

Further supporting these claims, disrupting awake SWRs via an online feedback system while a rat was learning a spatial task resulted in an impairment of learning performance. However, the place fields and the reactivation of SWRs during post-exploration session remained intact (Jadhav, Kemere et al. 2012). This research suggested that the replay during awake SWRs is also important for learning and memory. In another paper, experiments showed that when pyramidal cells in CA1 were optogenetically silenced when SWRs were detected at a rewarded location in the environment then place cells remapped, suggesting that the change of cell activity during SWRs impairs the stability of hippocampal spatial maps (Roux, Hu et al. 2017).

It is widely believed that spatial memory is slowly consolidated following encoding. Based on the evidence above, SWRs have been suggested as a mechanism of memory consolidation during the post-exploration rest periods, particularly for the systems consolidation of information between brain areas, for example from hippocampus to neocortex. As SWR-related neuronal activity is observed not only in hippocampus but also in prefrontal cortex, SWRs may mediate the communication between hippocampus and prefrontal cortex for reactivating information stored in both areas, leading to memory consolidation (Tang and Jadhav 2019). In addition to memory consolidation, SWRs are also thought to support memory retrieval, as the neuron active during SWRs can reflect or replay past experiences. This SWRs associated memory retrieval is also important for the consolidation during wakefulness and sleep (Joo and Frank 2018).

1.5 Cell assemblies

D. O. Hebb, a Canadian neuropsychologist, coined the term "cell assembly" to describe a group of neurons that are repeatedly activated during a mental phase, thereby strengthening the excitatory synaptic connectivity among its participants (Hebb 1949). The spatiotemporal component of the activity of its members defines a cell assembly. The term "cell assembly" is now widely applied to a group of cells in different areas of brain that conduct specific types of behavior or represent particular percepts. Normally, the assembly is thought to be a group of cells that have strong mutual synaptic transmissions that distinguish them from other groups of cells. In other words, it is assumed that the cell connectivity within an assembly

should be stronger than that among different assemblies. In hippocampus, it was found that place cells that had similar or overlapping place fields in a particular environment were more likely to be co-activated after the exploration than before it. This increased probability of co-activation was not observed in place cells that were inactive during behavior nor in those that were active without overlapping place fields. Similar to the classical Hebbian assemblies, it was shown that the newly formed cell ensembles were reactivated preferentially during high frequency SWRs, again supporting the long-held idea that offline SWR reactivation plays an important role in the consolidation of memory-representing assemblies (van de Ven, Trouche et al. 2016).

To identify groups of cells that fire together on the track, researchers have developed algorithmic assembly detection approaches that do not require assumptions about place fields. In cell assembly analysis, principal component analysis (PCA) and independent component analysis (ICA) are applied to find groups of repeatedly co-active cells across all the recorded population (van de Ven, Trouche et al. 2016). Detection is done using data recorded during exploration, such as when an animal is running on a linear track, to identify groups of neurons that fire together within short time windows (Figure 1.6). The advantage of using this technique is that it is relatively flexible and does not require neurons always to fire exactly in the same order or for the same amount of time. Also, cells can drop out and not fire at all from time to time, but the assembly can still be identified. However, when the same assemblies are later tracked in a subsequent sleep session, changes in these factors will influence the overall strength of reactivation, a metric which quantifies activity and participation. As a result, if all the cells reactivate together all the time in the exact same manner, the strength of reactivation will be very high. In contrast, if cells are often dropping out or the temporal order drift, then the reactivation strength will be much lower. The co-firing of cells in each cell assembly was reported to facilitate the synaptic plasticity in downstream circuits, which is important for the strengthening and reinstatement of spatial memory (Langille and Brown 2018).

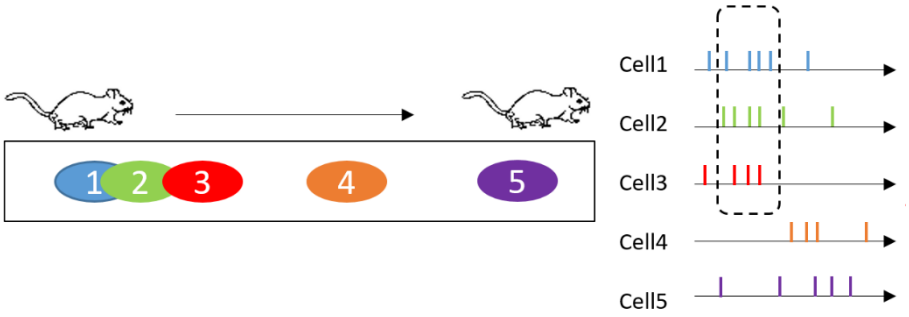

Figure 1.6 Cell assembly

1.6 Replay

1.6.1 Replay events

The study of Wilson and McNaughton (1994) was the first to look at experience-dependent reactivation of place cells during rest. In those experiments the authors recorded a large number of neurons during a sleep session before exploration, during exploration of a linear track, and then in a subsequent sleep session (Wilson and McNaughton 1994). They demonstrated that place cells with overlapping place fields on the track had strongly correlated activation in the subsequent sleep session, while no robust temporal correlations were observed in pairs with non-overlapping place fields. Notably, these temporal correlations were not present during a rest session prior to exploration, thus the increase was experience-dependent. Further, the strength of these pairwise correlations was much higher during SWRs than the interval between them. These results suggested that the re-activation of cell pairs enhanced the information formed during exploration, which was also thought to be a mechanism of memory consolidation.

Skaggs and McNaughton followed up on these findings by showing that the sequence of co-activated cells during exploration was preserved in the following resting session. And once again, the correlated activity of cells in sequence was stronger during the post-exploration session than that during pre-exploration session (Skaggs and McNaughton 1996). Hirase et al. in a later study found that a group of cells that was co-activate during exploration has a stronger correlation between the exploration and post-

exploration sessions than between the exploration and the pre-exploration sessions. This correlation of cells decreased when new cells were recruited as the animal explored a novel environment. Consistent with the previous research, they suggested that the neural co-activation can result in a long-term modification of synapses during high frequency oscillation, which is important for memory consolidation (Hirase, Leinekugel et al. 2001). However, the exact temporal structure of neuronal sequences cannot be described sufficiently by pairwise cross-correlograms, particularly when higher-order connections are involved. Replay sequences of place cells were first observed when animal was in the state of slow wave sleep (SWS) immediately after exploration (Lee and Wilson 2002). During the sequence, place cells fired in the same order as during exploring, however in a temporally compressed manner.

Replay was also observed in awake animals, especially during periods when the animal is standing still. During awake SWRs, which occur when the animal pauses its behavior, the sequence of place cell activations seen during exploration were replayed in both the forward and reverse directions. Foster et al. found the replay sequences of place cells when animal was consuming reward at the end of a linear track after exploration (Foster and Wilson 2006). The place cells reactivated in a reverse order of the behavioral sequence, starting from the end of the track and extending to the beginning, and were enriched immediately following spatial navigation. Thus, the sequential reactivation of hippocampal place cells that reflects previously experienced behavioral trajectories was also reflected in these reverse replay events. For example, Figure 1.7 demonstrates when animal explores on a linear track, Cell 1 to Cell 6 fired in specific locations on the track in a sequential way. Then, the same cells fired in the reverse order when the animal was resting in the post-exploration session during SWRs.

The forward replay of place cell sequences prior to the exploration of familiar environments has been suggested to play a role in anticipation of the following exploration (Diba and Buzsáki 2007). Furthermore, the firing sequences of place cells in a novel environment also takes place during resting before exploration of a context where the animal has yet to visit. This phenomenon is called preplay, as the temporal sequences occurred before the actual exploration of the novel environment, suggesting that the hippocampus plays a

role in prediction, which is thought to be helpful for accelerating the formation of novel memory (Dragoi and Tonegawa 2011).

As it has been proposed that the consolidation of memory involves transfer of information from hippocampus to other cortical areas, this repeated reactivation of sequences might mediate the consolidation of memory in other brain areas during sleep or pauses in behavior. Furthermore, sensory input may affect the details of replay, implying that awake replay also plays a role in memory retrieval (Derdikman and Moser 2010, Dupret, O'Neill et al. 2010, Ólafsdóttir, Bush et al. 2018).

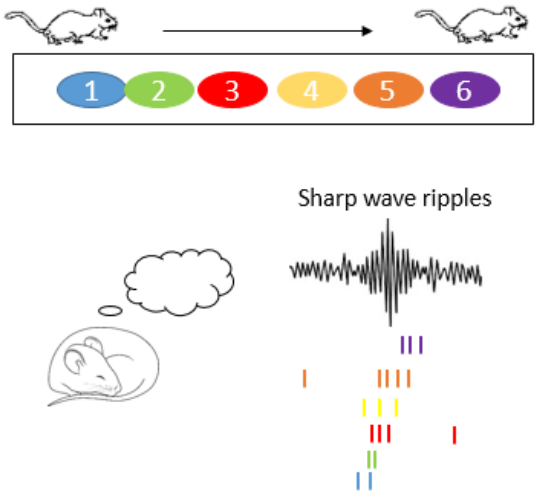

Figure 1.7 Replay event

1.6.2 Bayesian replay analysis

Bayesian decoding of replay activity uses all the spikes of neurons active during the SWRs period and relies on the pattern of place cell activation in the previous exploration session as its prior, thus is considered to be an efficient approach for detecting sequential reactivation. This approach uses the ensemble spiking in defined time bins during SWR events, which is used to estimate a series of decoded positions for each bin based on the average spatial firing of each given neuron in the environment (the prior) (Davidson,

Kloosterman et al. 2009, Karlsson and Frank 2009). In general, if the trajectory of decoded positions is more similar to the actual sequences observed across the place fields than trajectories constructed from temporally shuffled data, then the event is considered to be a significant replay event. It is essential that the shuffling algorithm be memoryless, meaning that every temporal bin of the sharp wave ripple is decoded independently, in order to prevent temporal smoothing over neighboring decoded positions, which would lead to the detection of false positive trajectories.

In order to better understand how to identify replay events I will explain the above in more detail. First, SWR events are detected. Analyses are often restricted to periods when the animal is not moving and the theta to delta ratio is relatively low in order to separate the replay events from the sequential spikes which occur during phase precession related to movement within each theta oscillation. SWRs are then spilt into time bins that cover a single oscillation cycle, all spikes from all neurons are taken and the Bayesian analysis is used for decoding. The activity of place cells in each temporal window is used to generate virtual positions according to smoothed firing positions of place cells during previous exploration as a template. A sequence score is calculated according to the Bayesian estimation of probability of the animal's location based on the preferred firing locations of cells. If the probabilities show a smooth trajectory across space over time, the sequence score is higher, while, if the positions are random, i.e., jumping back and forth on the track, the sequence score is lower.

1.6.3 Per cell contribution for each replay event

As explained above, replays are decoded based on the firing rate of several place cells during SWRs and a sequence score of each replay event can be formed by calculating the weighted correlation of probability of the animal location based on the preferred firing locations of cells. As the replay events involve several neurons, the sequence score can be differentially influenced by the activity of each neuron, thus the identification of each neuron's contribution to replay events is useful to address the lateralization of hippocampal neurons in the sequential reactivation of neural activity. In the paper published by Grosmark et al., the term "Per Cell Contribution (PCC)" was first employed to describe the contribution of each place

cell to a given sequence, with neurons with high PCC scores making large contributions to the observed sequence information (Grosmark and Buzsaki 2016).

Calculating the PCC score is based on measuring the decrease in the sequence score of replay events between the observed sequence score and the score following shuffling the spikes of a single given cell. The difference of sequence scores is then normalized by the number of neurons that participate in this event. The larger the drop in sequence score, the higher the contribution of that neuron to the sequence. For example, in Figure 1.8, in order to calculate the contribution of Cell 6 to the replay event, the observed sequence score was calculated first. Then the cell 6 location is shuffled, and shuffled sequence score of the same event is calculated again. The difference between the observed and averaged shuffled weighted correlation is the contribution of this cell to this replay event. The bigger the difference, the larger is the contribution of this cell.

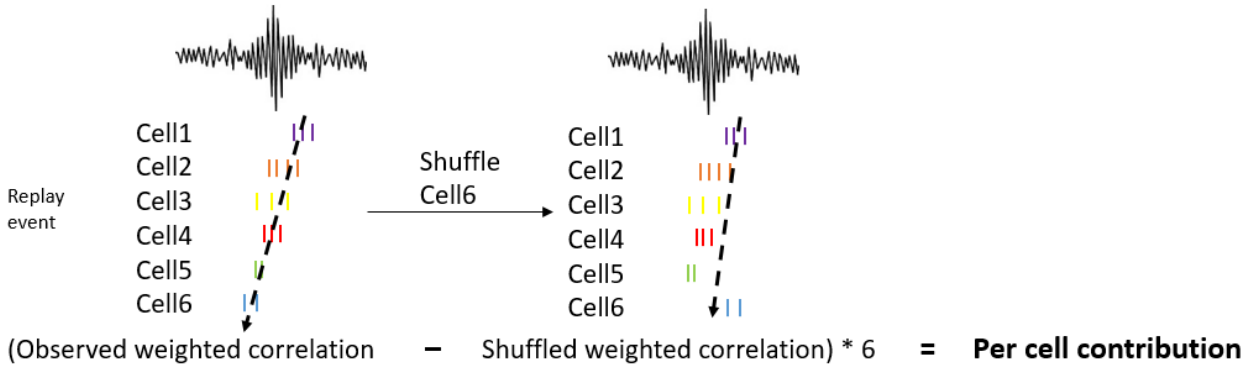

Figure 1.8 Per Cell Contribution (PCC) calculation.

1.7 CA3-TeTX mice

The CA3-TeTX mouse line was first developed by Nakashiba and colleages at MIT and carries three independent transgenes which together allow the inducible expression of the light chain of the tetanus toxin (TeTX) specifically in CA3 pyramidal cells (Figure 1.9; (Nakashiba, Young et al. 2008). The mutant mice are heterozygous triple transgenics and the control littermates are heterozygous double transgenics, lacking

the transgene cassette containing Cre-dependent switchable tetracycline transactivator (tTA) gene. TeTX is an endoproteinase specific for cleavage of VAMP2 (Schiavo, Benfenati et al. 1992) which is necessary for synaptic vesicle fusion required for neurotransmitter release (Schoch, Deák et al. 2001). In the mutant mice, synaptic transmission mediated by VAMP2 is blocked by the expression of TeTX, which can be turned on by removing the drug doxycycline (DOX) from the animal's diet (Nakashiba, Young et al. 2008). In comparison to the restricted knockout of the N-methyl-D-aspartate (NMDA) receptor gene NR1 within hippocampus, which results in mice lacking NMDA receptor-mediated synaptic currents and long-term potentiation in CA1 synapses, this method, blocking synaptic transmission, enables a complete and inducible silencing of chemical neurotransmission from all axons originating from targeted cell population (Tsien, Huerta et al. 1996, Nakazawa, Quirk et al. 2002, Nakazawa, Sun et al. 2003, McHugh, Jones et al. 2007).

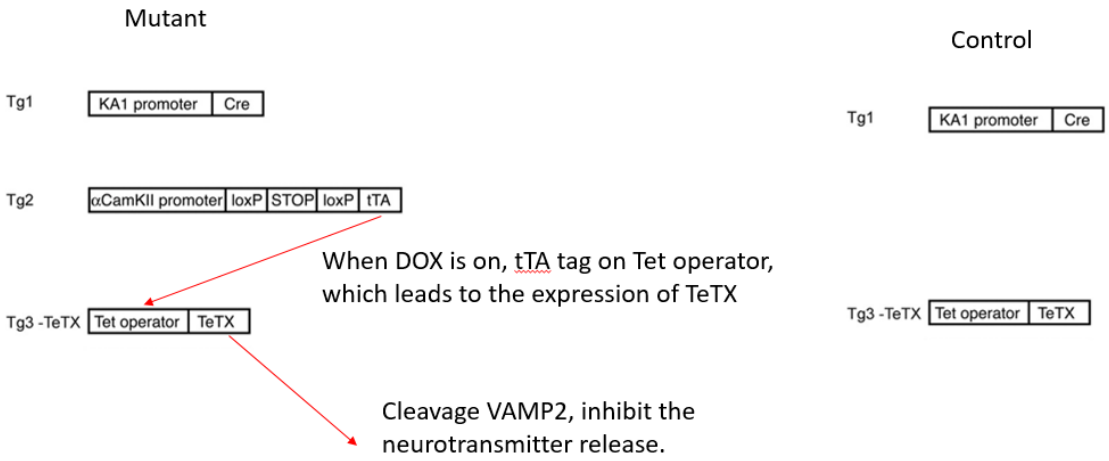

Figure 1.9 CA3-TeTX mice is a triple transgenic mouse line.

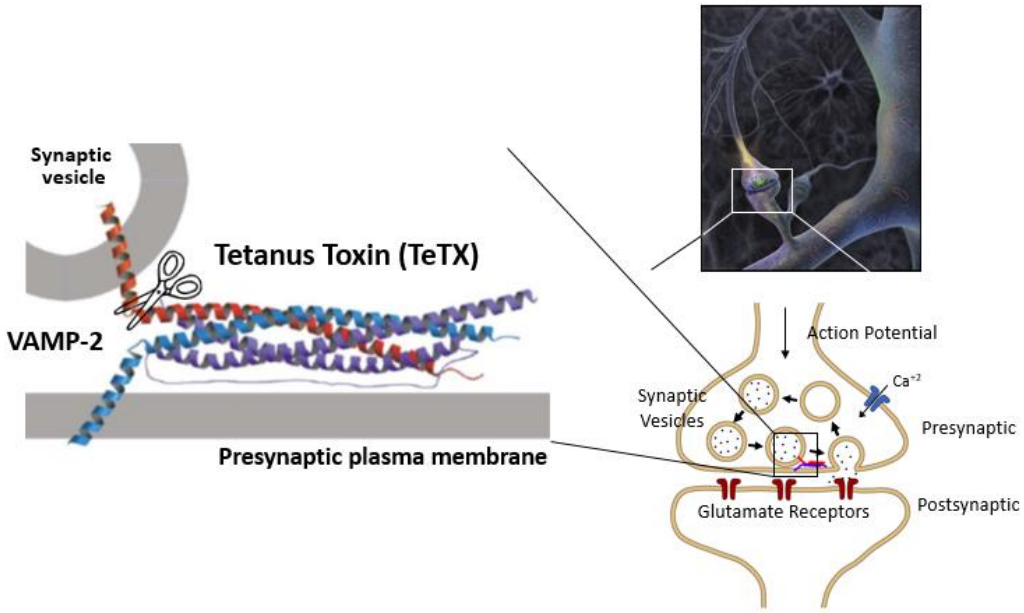

Figure 1.10 Tetanus Toxin blocks neurotransmitter release.

In CA3-TeTX mice that were raised on DOX containing food, replacing the DOX containing food with normal chow for four weeks results in a dramatic decrease of the VAMP2 protein in SR and SO of CA1 and CA3 (Figure 1.11), visualized with immunofluorescence staining using antibody against VAMP2. These results indicate that the blockade of synaptic transmission mediated by TeTX is both inducible and reversible in adult mice.

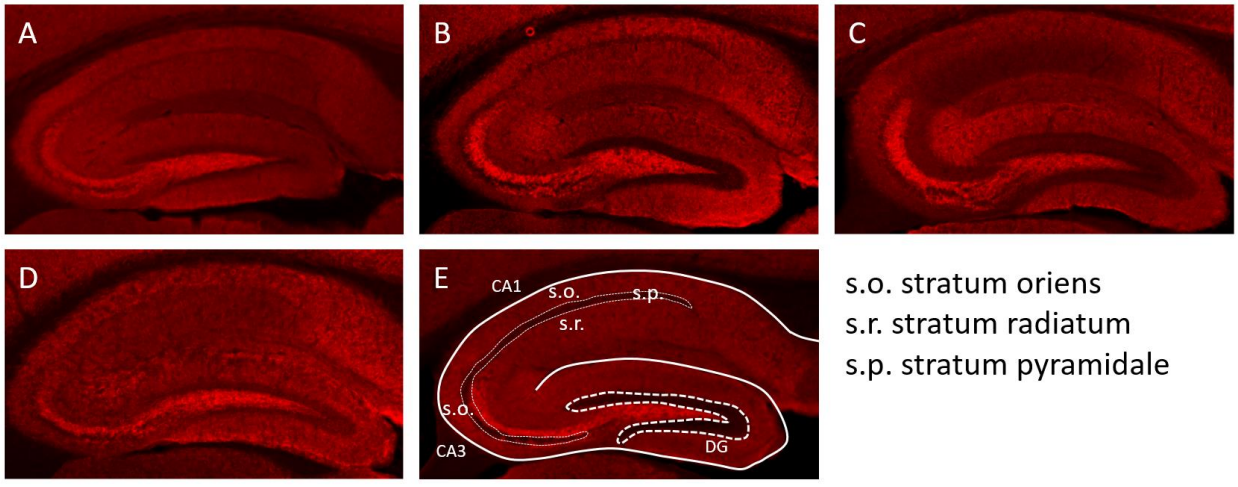

Figure 1.11 Expression of VAMP2 in the slices of CA3-TeTX mutant and control mice.

(A) A section from a control mouse. (B) A section from a mutant mice with DOX food all the time. (C) A section from a mutant mice following four weeks of normal chow, clearly shows a loss of VAMP2 in hippocampus. (D) A section from a mutant mice, which underwent 2 weeks of Dox withdrawal and then followed by 6 weeks of Dox re-administration. The VAMP2 immunoreactivity (IR) was similar to that in control. (E) Shows the location of various hippocampal strata. (Image courtesy of Thomas Mchugh (unpublished data))

1.8 Previous research and unanswered questions

1.8.1 Previous research using CA3-TeTX mice

In this study my experiments were built on past work with CA3-TeTX mice which I will review below.

Nakashiba et al. developed the CA3-TeTX transgenic mice to enable the reversible blockade of CA3 output by the relatively simply manipulation of changing the animal's diet. TeTX expression in CA3-TeTX mutant mice resulted in a dramatic loss of synaptic transmission from CA3 pyramidal cells, shown by slice recordings. Since there was no difference in the recall of spatial memory, it was concluded that CA3 output plays an important role in the acquisition of memory in a novel context, as well as the pattern-completion based recall of a previously formed contextual memory. In this study in vivo electrophysiology was also conducted and it was found that when the mutant mice explored a novel track the spatial tuning and spatial information of pyramidal cells in CA1 was significantly lower than in control mice. Overall, this paper suggested that CA3 output is essential for both rapid memory acquisition in new environments and recalling an already formed memory in an associative manner (Nakashiba, Young et al. 2008).

Later, Nakashiba et al. employed the same CA3-TeTX transgenic mice to examine the role of CA3 transmission in memory consolidation. They observed that the consolidation of contextual fear memory was impaired by the post-training blockade of CA3 output, suggesting that CA3 output is critical for memory consolidation. Consistent with these behavioral experiments, they found a reduction in the intrinsic frequency of SWRs in the mutant mice. Moreover, in the mutants, cell pairs in CA1 with overlapping place fields during exploration also showed a dramatic reduction in SWR-related co-firing in the post-exploration

sleep session. In total, they suggested that the CA3 output during post-training is needed for the coordinated reactivation of cell pairs during SWRs, a putative mechanism for the consolidation of contextual memory (Nakashiba, Buhl et al. 2009).

Recently, Middleton et al. found that, although the firing rate and temporal coding of pyramidal cells in CA1 during exploration were similar at the single cell level, the temporal coding at the cell population level (theta sequences) in CA1 was abolished by the blockade of CA3 output using the CA3-TeTX mice (Middleton and McHugh 2016).

All the studies introduced above using the CA3-TeTX mice adopted in vivo electrophysiological recording within CA1 in a single hemisphere (the right hemisphere) and investigated the role of CA3 input at both the single neuron level and the population level in CA1. However, simultaneous recording from bilateral CA1 had not been attempted in these mice. It is still not very clear if there is lateralization in rodent hippocampus, as so far almost all lateralization research has focused on in vitro electrophysiology, protein expression and behavior. While there are several in vivo physiological studies that mention hippocampal lateralization, reporting both bilateral hippocampal integration of spatial information (Carr, Karlsson et al. 2012, Pfeiffer and Foster 2013) and more directly, a lateralization in gamma band power (Benito, Martín-Vázquez et al. 2016), a careful and complete examination of the physiological properties at both the single cell and population level across the hemispheres in freely behaving rodents is absent. Further, no previous work has employed interventional approaches to address the circuits responsible for the integration of spatial information across the left and right hippocampi. As the brain works as a whole and there are dense connections within it, in vivo electrophysiology recording in the intact brain is necessary for a full understanding of integrated circuit function. Furthermore, previous in vitro research has suggested that the lateralization of rodent hippocampus may be most related to the input from CA3 (Song, Wang et al. 2020). As a result, in my study, I focused on the lateralization of hippocampus by turning off CA3 input using the CA3-TeTX mice.

In addition, due to the technical difficulty in recording a sufficient number of neurons simultaneously in the mouse brain, the role of CA3 input in the replay of place cells in bilateral CA1 remains unclear: the Bayesian decoding analysis of replay requires large ensembles of neurons recorded simultaneously (Carr, Jadhav et al. 2011). Here I took advantage of the development of better tools and parts for building in vivo recording microdrives to record large population of neurons simultaneously from bilateral CA1, allowing me to extend the earlier works on pairwise activity correlation analysis during ripples (Nakashiba et al 2009) and to assess the effect of silencing the CA3 input on replay in bilateral CA1.

1.8.2 Silencing bilateral CA3 input by optogenetic tools in mice resulted in a dramatic decrease of SWRs and replay in unilateral CA1.

In a study published by Yamamoto et al. (Yamamoto and Tonegawa 2017), AAVrh8-hSyn1-DIO-eArchT-eYFP, a viral construction that permits expression of the inhibitory opsin ArchT only in Cre expressing cells, was injected bilaterally into the CA3 region of CA3-Cre mice. ArchT is a light-activated proton pump that is frequently used to inhibit neural activity when triggering by green-yellow light. Optical stimulation of synaptic terminals of CA3 neurons in bilateral CA1 inhibited synaptic transmission and unilateral recording from right side of CA1 was performed. Distinct from the result of silencing CA3 genetically with TeTX, transient optogenetic silencing led to a dramatic decrease in the occurrence of SWRs during light stimulation. Further, the authors observed a significant decrease in replay events during light stimulation in the right CA1. As only CA1 in the right hemisphere was recorded, it was not possible to address the importance of CA3 transmission to the bilateral CA1 and the coordination between the hemispheres.

1.8.3 Silencing bilateral CA3 input by optogenetics tools in rat impaired SWRs and quality of replay in bilateral CA1.

In a recent study it was suggested that acute optogenetic silencing of CA3 resulted in a decrease of the occurrence of SWRs and replay quality in bilateral CA1 of rats (Davoudi and Foster 2019). Moreover, they

showed that the cell responses to the terminal silencing of CA3 input were not consistent in CA1. Even in cells recorded on the same tetrode, single cell responses were variable, including activation, inhibition and no change in firing rate. Although bilateral CA1 neurons were recorded with bilateral CA3 silenced, left and right CA1 neurons were not compared directly and the relationship between left and right CA1 neural activity were not investigated.

Consistent with the data of Yamamoto et al., a dramatic decrease in the occurrence of SWRs in CA1 during optogenetic silencing of CA3 was reported (Yamamoto and Tonegawa 2017); again a phenotype distinct from that of CA3-TeTX mice which showed no change in SWRs occurrence (Nakashiba, Buhl et al. 2009). Moreover, responses of single place cells were not consistent between the CA3-TeTX mice and CA3-ArchT expressing rats as well, leaving open questions concerning how the replay of bilateral CA1 place cells would look like in the CA3-TeTX mice and the consistency of chronic silencing with the transient silencing in the Davoudi's paper.

These inconsistencies most likely stem from the fact that Davoudi et al. and Nakashiba et al. used different techniques for silencing CA3 input into CA1. In the former, optogenetics was applied to acutely silence the CA3 input in CA1 by applying light to the CA3 terminals. However, the expression of the light-activated channel (ArchT) by viral transfection lacked cell-type or brain region specificity, in contrast to the CA3 pyramidal cell specific silencing in the study of Nakashiba et al.. Thus, neurons not only in CA3 but also in other brain regions, namely CA2, could have been inhibited. Furthermore, although they did injected in several locations in bilateral CA3, it is not possible to gain equal viral expression along the entire CA3 axis, which could lead to an incomplete inhibition of input from CA3. In my personal opinion, this might be one of the reasons why they saw a heterogeneity of neuronal responses in CA1. In addition, as there is a limitation for the size of optic fiber in optogenetics experiment, as well as the imbalance of light intensity that cells receive due to the different distance of cells from optic fiber, the silencing of CA3 input is not well distributed.

In the CA3-TeTX transgenic mice, issues discussed above do not exist, as the CA3-specific promotor-driven transgenic gene expression allows the complete silencing of bilateral CA3. The similar amplitude of SWRs seen in the CA3-TeTX mice might be attributed to the contribution of CA2 in SWR generation and reactivation of assemblies, even when CA3 is intact (Oliva, Fernandez-Ruiz et al. 2016, Oliva, Fernandez-Ruiz et al. 2020). In the study of Oliva et al. published in 2016, when recording from all CA subregions, it was found two patterns of pyramidal cells in CA2 fired before the bursting observed in CA3. Both the cells in deep and superficial layer of CA2, which were termed ramping cells and phasic cells respectively, showed an increasing firing rate prior to SWRs in CA3. This activity could then subsequently be observed propagating across CA3a, CA3b, CA3c and finally CA1, with a temporal delay. Moreover, in a second study from Oliva et al., published in 2020,the authors demonstrated structured reactivation of socially active neurons during these CA2 SWR events, as well as evidence indicating that manipulation of these events affected memory function.

In conclusion, considering the difference of approaches employed for CA3 silencing, as well as the difference of species and the different conclusions related to the occurrence of SWRs, I was interested in examining how replay looks like across bilateral CA1 following transgenic silencing of CA3 in mice. In addition, given that there is evidence of lateralization in receptor expressions, in vitro electrophysiology, and behavior, related to the CA3-CA1 circuit, I also wondered whether there is lateralization in the bilateral hippocampal circuit, especially for CA3-CA1 projection, when mice explored freely in familiar environment and during rest afterwards.

2 Materials and Methods

2.1 Subjects

Five CA3-TeTX transgenic male mice (Nakashiba, Young et al. 2008) and four male control littermates, all aged between 16 and 24 weeks were used in this study. All mice were bred and genotyped as previously reported (Nakashiba, Young et al. 2008). All mice were kept with the following method: both before and after birth pregnant dams were given water containing DOX (doxycycline hydrochloride, MP Biomedicals LTD) with the concentration of 10 μg/ml and sucrose with the concentration of 1% (wt/vol, Nacalai Tesque). After weaning, all mice were given Dox containing chow food with a concentration of DOX 10 mg/kg (Bioserve). It has been shown that the diet described above is sufficient to suppress the expression of TeTX, and consequentially maintains the function of VAMP2. All mice for experiment were kept on a cycle of 12 hours daytime and 12 hours night time, with food and water freely available. The mice were maintained on doxycycline (10 mg/kg) containing diet from conception until 3 weeks after birth before the microdrive implantation surgery. At the time they were switched to normal chow to allow transgenic expression of tetanus toxin (TeTX) in pyramidal cells in CA3. All procedures described above were approved by the RIKEN Institutional Animal Care and Use Committee.

2.2 Surgery and recording preparation

A custom micro-drive (Figure 2.1(Kloosterman, Davidson et al. 2009) was fabricated with two separate bundles, 2.5 cm apart from each other, with each bundle containing eight tetrodes glued into a linear array, in which each tetrode is independently adjustable prior to recording (Figure 2.2). One day before the implantation surgery, tetrodes were gold plated until the resistance ranged from 175-250 kΩ. During surgery, the microdrive was implanted over CA1 bilaterally, with the center of each bundle targeted at -1.94 mm posterior and ±1.25 mm lateral to Bregma (Figure 2.3). Eight adjustable recording tetrodes were implanted in left and right CA1, respectively. The positions of individual tetrodes were confirmed via electrolytic lesion (Figure 2.4). The lesions (arrows) show the location of recording tetrodes at equivalent

positions in dorsal CA1 in both hemispheres. Following a recovery period of two days after surgery, tetrodes were independently slowly lowered towards the CA1 pyramidal layer to maintain the stability of all tetrodes. It has been noted that fast adjusting of tetrodes may lead to unexpected drift. Recording was started when all tetrodes were in the pyramidal cell layer, which was evident by large amplitude spikes of pyramidal cells as well as spontaneously occurring SWRs when animal was standing still.

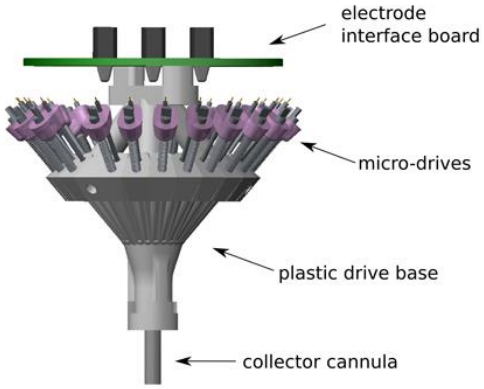

Figure 2.1 Micro-drive array.

Reuse from Kloosterman, Davidson et al. (Kloosterman, Davidson et al. 2009) with explicit permission from JoVE, the Journal of Visualized Experiments.

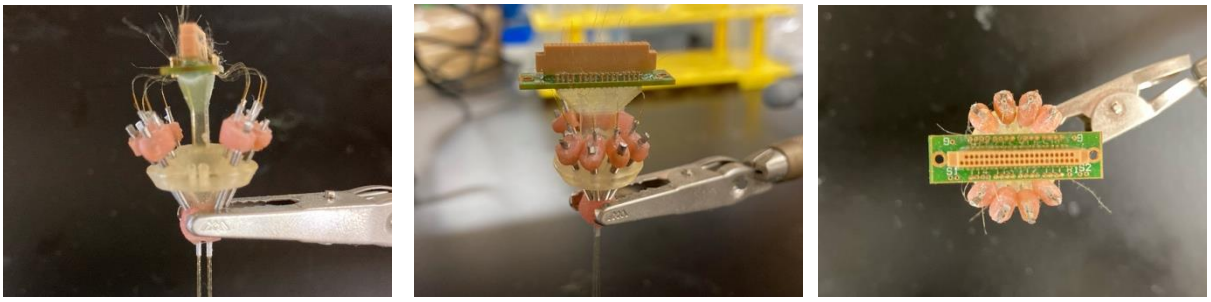

Figure 2.2 Different views of an example micro-drive prior to implantation surgery.

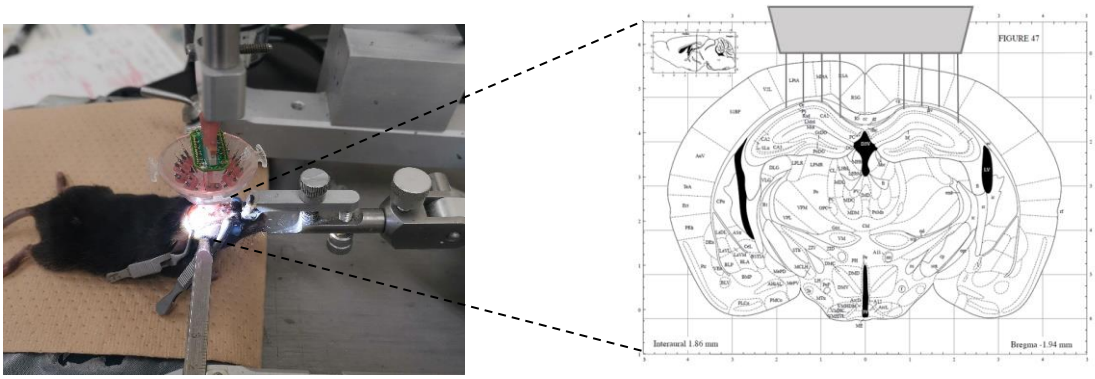

Figure 2.3 An example of implantation surgery.

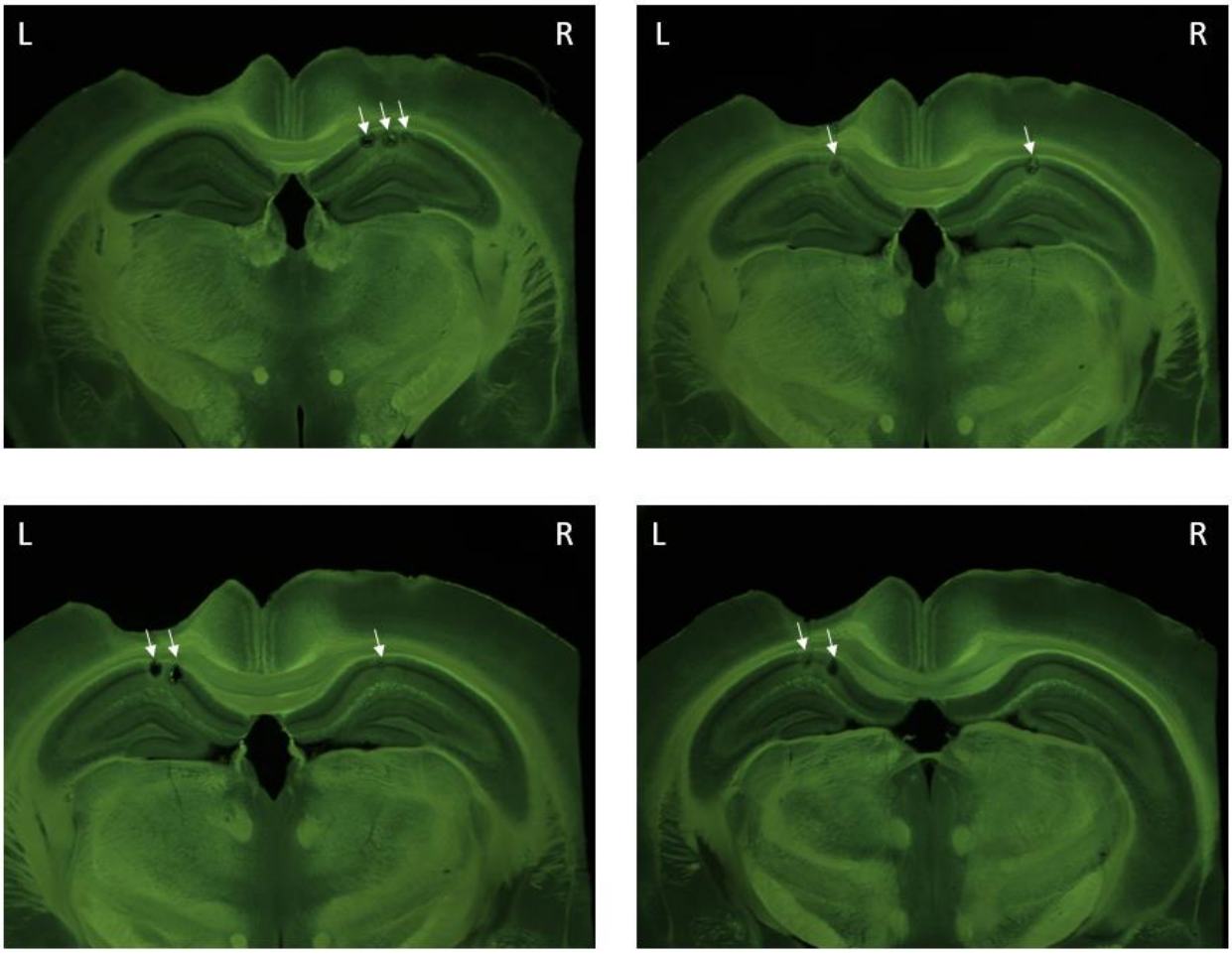

Figure 2.4 Histology shows tetrode locations in left and right hippocampal CA1. This figure was reproduced from (Guan et al. 2021).

2.3 Recording protocol

Data were collected with a 32-channel Digital Lynx 4SX acquisition system (Neuralynx) sampled at 32,556 Hz. Spike waveforms with frequency out of 0.6–6 kHz were filtered out. During the implantation surgery, a stainless steel screw was anchored in the skull above the cerebellum, which was used as ground. Tetrodes implanted in the corpus callosum were used for reference. Three recording sessions were conducted over the course of a single day. First, animals were put in a highly familiar small box with a wall high enough to shut out the environment (sleep box) for 1 hour to ensure stability of single unit recording. Then, animals were placed on a familiar linear track with opaque walls of the size 150 cm (length), 15 cm (width), and 15 cm (height). Animals could freely explore the linear track, moving from one end to the other, and recordings continued until either 20 laps had been completed or 20 minutes had elapsed. Animals were then immediately transferred back to the same sleep box and kept for 1 hour. The positions and the direction of animal's head were tracked throughout all three sessions using a pair of red and green light emitting diodes put on left and right side of the recording drive respectively and monitored by a ceiling mounted camera.

After completing the recording sessions each mouse was anesthetized and the brain tissue was lesioned by electric current (50 μA) for 10 s passed down each tetrode to label the location of recording tetrodes. Immediately after lesioning, transcardial perfusion was performed with 4% paraformaldehyde (w/v) (PFA), then brains were removed and immersed in 4% PFA for 24 h. Fixed brains were sliced coronally with a vibratome (Leica) with the thickness of 50 μm and the location of tetrodes were confirmed with standard light microscopy.

2.4 Place cell analyses

2.4.1 Cell cluster and pyramidal cell classification

SpikeSort3D software (Neuralynx) was used to cluster cells based on recorded waveform parameters, spike amplitude and energy (which is the square of the signal) of the waveform. Putative cells were manually identified by tracing a 3D boundary around the spikes within these representations, assuring no overlap with the spikes of any other putative single neuron. (Figure 2.5).

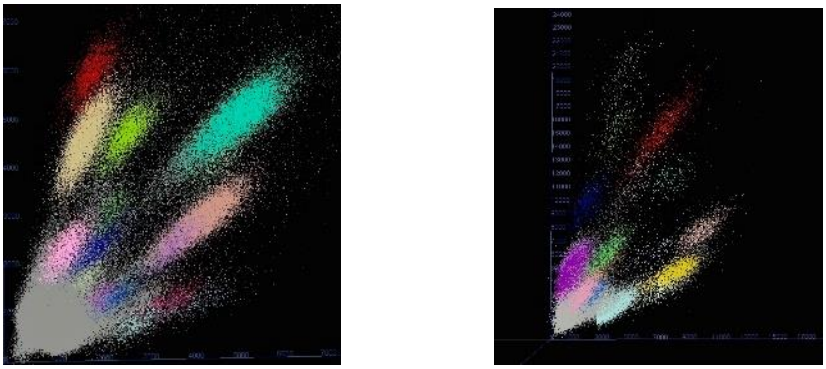

Figure 2.5 2D views showing clustered neurons of two different tetrodes.

Each dot represents a single neural spike recorded in a single session. Different colors represent different neurons, the spikes with the same color belong to one single neuron.

In order to compare the same group of cells across the 3 sessions, cells were first clustered in the last rest session data and the resulting cluster boundaries were applied to the first two sessions. Clusters with over 0.5% of spikes displaying interspike intervals less than 2 ms, containing less than 75 total spikes or having an isolation distance from other clusters less than 20 (Schmitzer-Torbert, Jackson et al. 2005) were discarded. The remaining cells, of which average spike width over 200 μs and complex spike index (CSI)(McHugh, Blum et al. 1996) over 5, were classified as putative pyramidal cells. A velocity threshold of 5 cm/sec was then applied to the data on the linear track and any cells with less than 75 spikes during periods of movement were also discarded.

As mentioned above, the complex spike index (CSI) was used to distinguish pyramidal cells from interneurons. It is known that the pyramidal cells fire in burst, which can induce synaptic plasticity in the downstream area receiving projections from those pyramidal cells. However, some interneurons can also fire burst, however with different burst properties. In pyramidal cells, interspike intervals are shorter, and the amplitude of successive spikes are lower. CSI is defined as the percentage of spike pairs with interspike interval between 2 ms and 15 ms and the amplitude of second spike smaller than the first one (McHugh, Blum et al. 1996). It was shown that the CSI of pyramidal cells was much higher than that of interneurons, thus CSI can be used to distinguish the cell type.

2.4.2 Definition of place cells properties

Firing rate on the linear track is defined as the total spike number of each cell divided by the total time that animal spent on the linear track. **Firing rate in rest** is defined as the total spike number of each cell divided by the total duration of the rest session. **Firing rate in SWRs** is defined as the total spike number of each cell during ripples divided by the sum of ripple durations in rest session.

2.4.3 Spatial Information

Spikes of each place cell were separated into two groups according to the direction of the animal's movement. The position at which spikes occurred was determined by dividing the track into 100 equally sized bins, and the resultant spike map was smoothed with a Gaussian smoothing kernel (S.D. = 5 cm). A firing rate map was derived by diving the smoothed spike map by the occupancy map, which was calculated as the cumulative time the animal spent in every spatial bin of the linear track, and was smoothed with the same Gaussian smoothing kernel. Spatial information was calculated as previously described (Skaggs, McNaughton et al. 1996):

$$\text{Spatial information} = \sum_i p_i \frac{li}{l} \log_2 \frac{li}{l} \qquad (2.1)$$

Where i is a spatial bin, p_i is the probability of each mouse staying in that bin, l_i is the mean firing rate in that bin, l is the mean firing rate of the neuron.

2.5 Cell assembly analyses

2.5.1 Assembly pattern identification

Cell assemblies were detected to identify place cells that activate at the same time while the mice were exploring the familiar linear track using previously described methods (van de Ven, Trouche et al. 2016). The spiking activity of each neuron was separated into left and right directions according to the movement direction of the animal, temporally binned into 25 ms windows, and the number of spikes in each bin was calculated and normalized with a z-score transform. Next, the z-scored spike time matrix (Z) was calculated with Principal component analysis (PCA):

$$\sum_{j=1}^{n} l_j p_j p_j^T = \frac{1}{n} Z Z^T \tag{2.2}$$

Where p_j is the j^{th}principal component, and the l_j is the corresponding eigenvalue, and $\frac{1}{n} zz^T$ is the correlation matrix of Z. The number of significant patterns were estimated by the Marčenko-Pastur law, which is for an n × B matrix, the eigenvalues are expected to exceed l_{max}, if the neuron activity are thought to be independent from other cells (Peyrache, Benchenane et al. 2010). Here l_{max} is defined by

$$l_{max} = (1 + \sqrt{n/B})^2 \tag{2.3}$$

The number of eigenvalues above l_{max}, which shows the number of distinct significant patterns was defined as N_A. The significant principal components were projected onto the binned spike time matrix (Z):

$$Z_{PROJ} = P_{SIGN}^T Z \tag{2.4}$$

Where P_{SIGN} is an n $\times$ N_A matrix, and the columns are filled with first N_A principal components. Next, the matrix Z_{PROJ} was calculated with independent component analysis (ICA), using the fastICA Matlab package. Each cell's weight within that assembly was determined with the unmixing matrix W, obtained from last step:

$$\mathrm{V} = P_{SIGN} W \tag{2.5}$$

Where the columns of V are the weight vectors of the assembly patterns.

2.5.2 Unilateral and bilateral assembly detection

Within each assembly pattern, neurons whose weight exceeded the mean weight of the population by two standard deviations was consider a member of the assembly. For each cell assembly, if the all member neurons belong to the same hemisphere (either left or right), this cell assembly was considered as a unilateral assembly. In contrast, if a cell assembly consisted of neurons belong to both left and right hemispheres, it was considered as a bilateral assembly. The observed ratio of unilateral assemblies was derived by the number of unilateral assemblies divided by the total number of assemblies when the animal was moving in each direction.

2.5.3 Shuffling of member neurons in each cell assembly

For the cell assemblies that were detected in each animal, each cell assembly was reconstituted by randomly assigning neurons that were recorded simultaneously in the animal, avoiding repetitive assignment of the same cell, and the ratio of unilateral assemblies in each animal was calculated as described above. This reconstitution was repeated for 1000 times, as a result, 1000 shuffled ratios of unilateral assemblies were obtained.

2.5.4 Tracking expression of assembly patterns over time

Assembly reactivation was evaluated after the identification of cell assemblies in the exploration session, as follows:

$$R_k(t) = z(t)^T P_k z(t) \tag{2.6}$$

Where $R_k(t)$ is the activation strength of assembly k at the time t, and $z(t)$ is the z-scored binned spike time convolved with the Gaussian kernel. P_k is the pattern k which is projected from the matrix, and the outer product of its weight vector v_k was used and the diagonal entries were set to zero. Assembly strength was then calculated as the averaged strength of each assembly's pattern activations, with only peaks in the

expression strength exceeding 5 included. Assemblies with the reactivation rate less than 0.01/s were excluded from the statistic test.

2.6 Ripple detection

SWRs were only detected when animal velocity was below 2cm/s. SWRs were firstly detected after filtering local field potential with a band-pass Hamming window filter (90–250 Hz) and the root mean square power was calculated in the ripple band. SWRs were defined as periods, beginning when peak power was detected as more than 5 S.D. over the mean value and terminating when the power decreased less than 2 S.D. Additionally, two ripple events were considered as one if their peaks were closer than 50 ms. Peak frequency was calculated using the multitaper method (Buhl, Harris et al. 2003).

2.7 Ripple synchronization

The start and stop time points of all detected ripple events were used to calculate the temporal midpoint of each event. A vector of these timestamps was constructed for each hemisphere with temporal midpoints of ripple events from one hemisphere as reference. The occurrence of ripple events in the other hemisphere was detected across a 200 ms window centered on each midpoint of events from the reference hemisphere with 1 ms bin size (shown in Figure 2.6). The resulting column vector represented the probability of ripple events stemming from the opposite hemisphere, which was then smoothed with a Gaussian kernel of a standard deviation of 4.

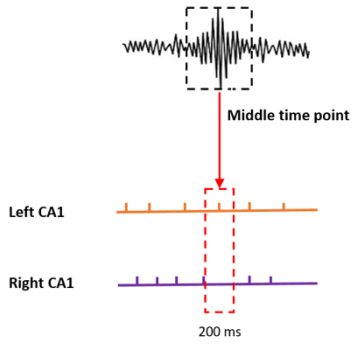

Figure 2.6 Calculation of the cross-correlation of SWR events from bilateral CA1.

2.8 Bayesian replay analyses

Spikes of each place cell were separated into two groups according to the direction of animal's movement. Only ripple events of duration between 50–300 ms with at least four participating place cells were included for the further analysis. Each ripple event was binned into non-overlapping 20 ms windows, and spike activity of place cells during the ripple event was calculated within those bins. The position of animal was deduced by decoding the activity of place cells in each ripple period with the Bayesian method (Davidson, Kloosterman et al. 2009), based on the smoothed firing rate of place cells during previous exploration:

$$\Pr(pos|spikes) = \left(\prod_{i=1}^{n} f_i(pos)^{sp_i}\right) e^{-\tau \sum_{i=1}^{n} f_i(pos)} \tag{2.7}$$

Where $f_i(pos)$ is the firing rate of the ith place cell template at the position pos, sp_i is the number of spikes of the ith place cell in the temporal bins which is decoded, τ is the period of decoding bins, and n is the total number of place cells. Then the posterior probabilities were normalized to one as follows:

$$\text{norm\_Pr}(pos|spikes) = \frac{\Pr(pos|spikes)}{\sum_{i=1}^{P_n} Pr(pos_i|spikes)} \tag{2.8}$$

Where P_n is the total number of positions.

Subsequently, a preliminary sequence score (r) was derived as the correlation of time and position for each event and weighted by posterior probability. First the weighted mean (m) was calculated as follows:

$$m(pos; \text{norm\_}Pr) = \frac{\sum_{i=1}^{M}\sum_{j=1}^{N} \text{norm\_}Pr_{ij} pos_j}{\sum_{i=1}^{M}\sum_{j=1}^{N} \text{norm\_}Pr_{ij}} \tag{2.9}$$

Next, the weighted covariance (cov) was calculated:

$$cov(pos, bin; \text{norm\_}Pr) = \frac{\sum_{i=1}^{M}\sum_{j=1}^{N} \text{norm\_}Pr_{ij}\left(pos_j - m(pos;\text{norm\_}Pr)\right)\left(bin_i - m(bin;\text{norm\_}Pr)\right)}{\sum_{i=1}^{M}\sum_{j=1}^{N} \text{norm\_}Pr_{ij}} \tag{2.10}$$

where pos_j is the jth spatial bin, $bin_i$is the ith temporal bin and $\mathrm{norm_}Pr_{ij}$is the posterior probability in the ith bin. M is the total number of temporal bins and N is the total number of spatial bins.

Then the weighted correlation $\mathrm{r}(pos, bin; \mathrm{norm\_}Pr)$ was calculated:

$$\mathrm{r}(pos, bin; \mathrm{norm\_}Pr) = \frac{cov(pos,bin;\mathrm{norm\_}Pr)}{\sqrt{cov(pos,pos;\mathrm{norm\_}Pr)cov(bin,bin;\mathrm{norm\_}Pr)}} \quad (2.11)$$

Next, the firing rate of each place cell template was circularly shuffled 1000 times. The activity of place cells in each window during each ripple event was then decoded again via the same method described above using the 1000 shuffled templates to generate 1000 shuffled weighted correlations (1000 r(null)). For each replay event, a sequence score (rZ) was calculated by the difference between the absolute value of the observed weighted correlation r(observed) and the absolute value of the averaged shuffled weighted correlation r (null), and normalized by the standard deviation of the absolute value of shuffled weighted correlation r(null):

$$\mathrm{rZ} = \frac{|r(observed)| - |\overline{r(null)}|}{s.d.(|r(null)|)} \quad (2.12)$$

In addition, in order to identify the quality of replay, a Monte Carlo P-value (Silva, Feng et al. 2015) was calculated for each event as follows:

$$P = \frac{(n+1)}{(r+1)} \quad (2.13)$$

Where r is the total times of shuffling (1000), n is the number of shuffling which has a weighted correlation over the observed value. As each event was decoded once for one direction of animal movement and another time for the other direction as well, only events with the smallest P-value, and only if that P-value was less than 0.05, were included for further analysis.

Mean jump distance was derived as the average distance between peak decoded positions of temporal bins that next to each other in each replay event. Replay distance was derived as the distance between the maximum and minimum of peak decoded positions in each replay event. Replay speed was derived as the replay distance divided by the duration that this replay event spent.

2.9 Per cell contribution (PCC) analyses

The place representation of each cell was randomly shuffled for 1000 times, in order to get shuffled matrices by calculating 1000 shuffled sequence scores for the particular cell. The per cell contribution of each cell (Grosmark and Buzsaki 2016) in each event was derived by calculating the difference between the observed sequence score of the event that the cell participated in ($rZ_e(observed)$) and the specific single cell shuffled sequence score of the same event ($rZ_{e,c}(cell\ c\ shuffled)$)), which is normalized by the number of participating cells in this event:

$$PCC_{e,c} = \left[rZ_e(observed) - rZ_{e,c}(cell\ c\ shuffle)\right] \times \#\ Participants_e \quad (2.14)$$

Where $\#\ Participants_e$ is the total number of place cells that were activated more than once in this event e. $rZ_e(observed)$ was derived as described above. For each cell that participated in the replay event, only the place representation for that specific cell was circularly shuffled 1000 times, and the average of this 1000 single cell shuffled sequence scores is the $rZ_{e,c}(cell\ c\ shuffle)$. The PCC of each neuron was defined as the neuron's mean contribution across all significant replay events.

2.10 Statistics

All data were analyzed with MATLAB R2019b. Wilcoxon rank sum test and unbalanced two-way analysis of variance (ANOVA) were applied to test the difference between groups. The Bonferroni test was used to conduct multiple comparisons between multiple groups for post hoc tests. Linear mixed effects models (LMMs) was applied to test the difference between left and right hippocampi, where mouse identity was specified as a random factor and left and right were specified as fixed factors. Results are shown in the way of mean ± S.E.M. All box plots show the distribution of data, with the central mark indicates the

median, the top and bottom edges of the box indicates 75th and 25th percentiles of the data, the whiskers represent the largest and smallest data points, in which outliers are not considered. Data are considered as outliers if they are bigger than q3 + 1.5 × (q3 – q1) or smaller than q1 – 1.5 × (q3 – q1), in which q1 is the 25th percentiles of the sample data and q3 is the 75th percentiles of the sample data, and the outliers are set invisible in order to make suitable visualization; **** indicates $P < 0.0001$, *** indicates $P < 0.001$, ** indicates $P < 0.01$, and * indicate $P<0.05$.

2.10.1 Wilcoxon rank sum test

T-tests are widely used for comparing the average and distribution of data between two groups, when the data can be assumed to be normal distributed. With in vivo electrophysiology data, theWilcoxon rank sum test is widely used as the data is not normal distributed. Furthermore, it has been suggested that data with outliers or of small size, Wilcoxon rank sum test is more proper than t-tests. According to the properties of the data set in this study, Wilcoxon rank sum test was employed.

3 Results

3.1 Pyramidal cell properties remain similar across bilateral CA1 after silencing CA3.

Given the unaddressed questions regarding the lateralization of spatial coding and assembly reactivation, as well as the underlying circuits involved, I designed experiments to specifically target the contribution of bilateral CA3 to CA1 transmission. I investigated the role of CA3 in organizing bilateral ensemble CA1 activity by genetically blocking synaptic transmission at CA3 terminals through the inducible transgenic expression of tetanus toxin (TeTX) and recording from bilateral CA1 in CA3-TeTX mice (Nakashiba, Young et al. 2008) and littermate controls, as mice explored a familiar linear track, as well as during flanking periods of rest (**Figure 3.1 a**). Consistent with previous reports (Nakashiba, Buhl et al. 2009), I observed that the mean firing rate (FR) of CA1 pyramidal cells (**Figure 3.1 b, c**) were similar in mutant (MUT) and control (CTR) mice during exploration (CTR, 0.40 ± 0.027 HZ; MUT, 0.46 ± 0.028 HZ) and during rest, both overall (CTR, 0.623 ± 0.053 HZ; MUT, 0.621 ± 0.038 HZ) and specifically during the occurrence of SWRs (CTR, 1.61 ± 0.171 HZ; MUT, 1.46 ± 0.095 HZ; **Figure 3.1 c**). However, the spatial information (SI) of CA1 place cells during exploration was significantly lower in the mutant mice compared to controls, reflecting the expected decrease in spatial coding in the absence of CA3 input (CTR, 0.87 ± 0.036 bits/spike; MUT, 0.79 ± 0.038 bits/spike; **Figure 3.1 d**).

I next compared the basic properties of place cells recorded in the left and right CA1 in control mice and in mutants following the silencing of CA3 input and found that the mean firing rate (FR) and spatial information (SI) during exploration were similar across hemispheres within both genotypes (FR: CTR L, 0.41 ± 0.036 HZ; CTR R, 0.39 ± 0.041 HZ; MUT L, 0.48 ± 0.040 HZ; MUT R, 0.44 ± 0.038 HZ; SI: CTR L, 0.87 ± 0.048 bits/spike; CTR R, 0.86 ± 0.055 bits/spike; MUT L, 0.70 ± 0.041 bits/spike; MUT R, 0.88 ± 0.063 bits/spike). The pyramidal cell firing rate (FR) during rest, as well as SWRs, also showed no evidence of lateralization in controls or mutants (FR in rest: CTR L, 0.55 ± 0.059 HZ; CTR R, 0.71 ± 0.095 HZ; MUT L, 0.66 ± 0.057 HZ; MUT R, 0.58 ± 0.050 HZ; FR in SWRs: CTR L, 1.43 ± 0.198 HZ; CTR R,

1.86 ± 0.304 HZ; MUT L, 1.63 ± 0.134 HZ; MUT R, 1.43 ± 0.149 HZ; **Figure 3.1 d**). Together, these data suggest that even in the absence of CA3 input, basic pyramidal cell firing properties remain similar across hemispheres.

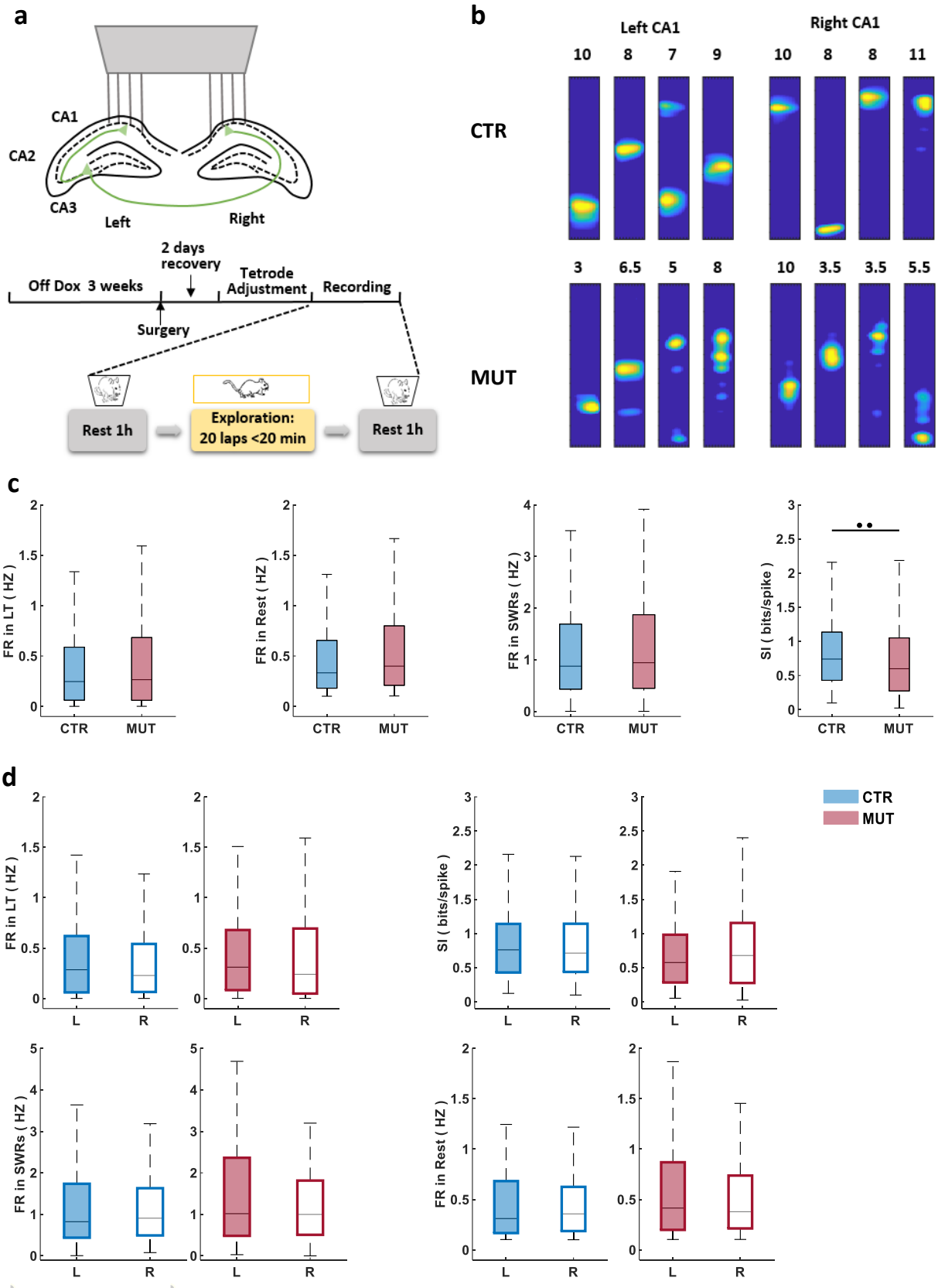
a
CA1
CA2
CA3
Left
Right
2 days recovery
Off Dox 3 weeks
Tetrode Adjustment
Recording
Surgery
Rest 1h
Exploration: 20 laps <20 min
Rest 1h
b
Left CA1
Right CA1
10 8 7 9
10 8 8 11
CTR
3 6.5 5 8
10 3.5 3.5 5.5
MUT
c
FR in LT (HZ)
FR in Rest (HZ)
FR in SWRs (HZ)
SI (bits/spike)
CTR
MUT
d
CTR
MUT
FR in LT (HZ)
SI (bits/spike)
FR in SWRs (HZ)
FR in Rest (HZ)
L
R

Figure 3.1 Pyramidal cell properties remain similar across bilateral CA1 after silencing CA3.

(**a**) Schematic representations of experimental protocols. Top: microdrive placement for bilateral CA1 recording; center: timeline of Dox food withdrawal, surgery and recording; bottom: structure of the recording day. (**b**) Representative examples of firing-rate maps on the linear track from left and right CA1 of controls and mutants. Colors are scaled to peak firing rate (Hz) indicated at the top of each map (blue, minimum; yellow, maximum). (**c**) Mean firing rate during exploration (CTR, N=4 animals, n=273 cells; MUT, N=5 animals, n=318 cells; P (mean firing rate during exploration) = 0.1939), rest and within SWRs was comparable between genotypes (CTR, N=4 animals, n=227 cells; MUT, N=5 animals, n=290 cells; P (mean firing rate during rest) = 0.1167; P (mean firing rate during SWRs) = 0.6285). Spatial information during exploration was significantly lower in mutants (CTR, N=4 animals, n=273 cells; MUT, N=5 animals, n=318 cells; P = 0.0046). (**d**) Pyramidal cells properties were comparable between left and right CA1 (Filled bars: left hemisphere; open bars: right hemisphere; CTR, N=4 animals, n (left) = 152 cells, n (right) = 121 cells; MUT, N=5 animals, n (left) = 162 cells, n (right) = 156 cells; mean firing rate during exploration: P (CTR) = 0.6816, P (MUT) = 0.1030; spatial information during exploration: P (CTR) = 0.6551, P (MUT) = 0.3257; during sleep: CTR, N=4 animals, n (left) = 126 cells, n (right) = 101 cells; MUT, N=5 animals, n (left) = 158 cells, n (right) = 132 cells; mean firing rate during rest: P (CTR) = 0.5773, P (MUT) = 0.5291; mean firing rate during ripple: P (CTR) = 0.2369, P (MUT) = 0.0676); significant difference in Figure 3.1d were tested with LMMs. Unless mentioned, all significant difference in Figure 3.1 were tested with Wilcoxon rank sum test. This figure was reproduced from (Guan et al. 2021).

3.2 Decrease in bilateral CA1 cell assemblies following the silencing of CA3 input.

Given that I observed no hemispheric differences in single cell spatial coding properties in CA1, I next asked how the loss of CA3 transmission impacted the bilateral co-activation of temporally coordinated cell assemblies. I identified the repeated neuronal co-activation of place cell assembly patterns from bilateral CA1 during exploration of the familiar track using a combination of principle component and independent component analyses and then tracked the activity of these assemblies over time (van de Ven, Trouche et al. 2016) (**Figure 3.2 a**). Assemblies were present in the mutant mice, and while no significant changes were observed in average assembly size between the genotypes (CTR, 3.19 ± 0.099 cells; MUT, 3.17 ± 0.116 cells; **Figure 3.2 b**), there was an increased fraction of neurons in the CA3-TeTX mice that did not belong to any assembly (CTR, 0.37 ± 0.025; MUT, 0.47 ± 0.040; **Figure 3.2 c).** Moreover, compared to the controls, the strength of assembly activation in the mutants was significantly lower during the exploration session (CTR, 343.50 ± 72.691; MUT, 142.41 ± 21.676). This decrease persisted during the rest session, where assembly reactivation strength was again significantly lower in mutants (CTR, 27.27 ± 1.825; MUT, 25.82 ± 2.724; **Figure 3.2 d**).

a

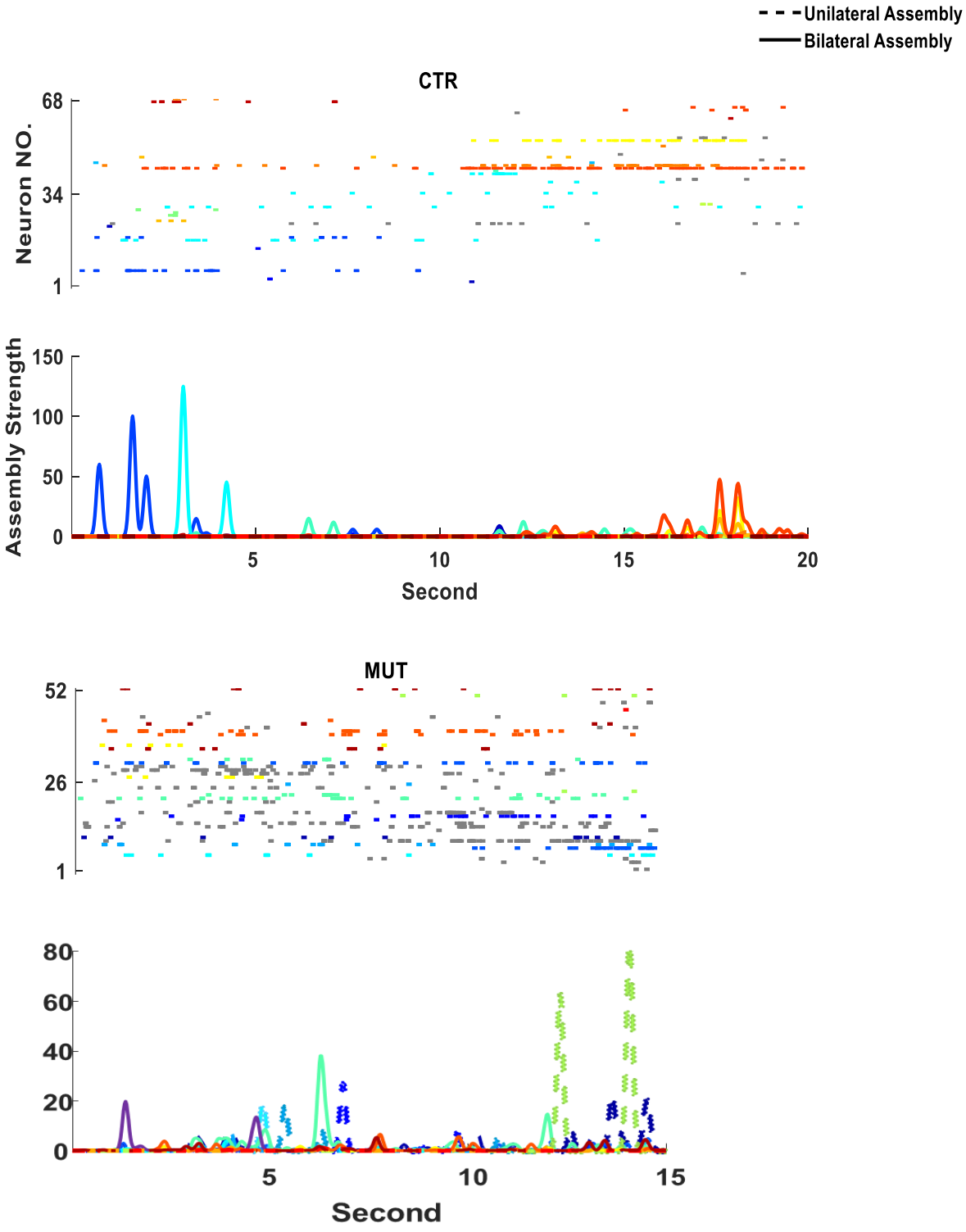
Unilateral Assembly
Bilateral Assembly
CTR
Neuron NO.
68
34
1
Assembly Strength
150
100
50
0
5
10
15
20
Second
MUT
52
26
1
80
60
40
20
0
5
10
15
Second

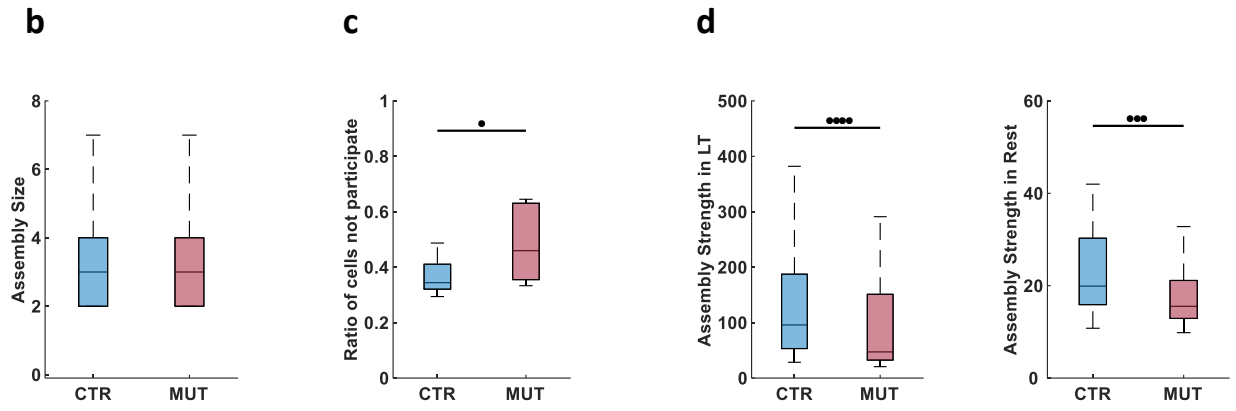

Figure 3.2 Silencing CA3 input decrease bilateral CA1 cell assemblies, but assembly size and participation keep similar.

(a) Top: example raster plots of simultaneously recorded pyramidal cell activity during a single lap on the linear track from one control (68 cells) and one mutant (52 cells) mouse. Cells of the same color belong to the same assembly, cells shown in grey do not participate in any cell assemblies. Bottom: strength of each cell assemblies (colors correspond to rasters above; CTR, 10 assemblies in total; MUT, 12 assemblies in total); solid lines represent assemblies containing cells from bilateral CA1 (CTR, 10 assemblies; MUT, 7 assemblies); dashed line represents unilateral assemblies (CTR, 0 assemblies; MUT, 5 assemblies). **(b)** Assembly size was similar in control and mutant mice (CTR: N=4 animals, n=123 assemblies; MUT: N=5 animals, n=121 assemblies; P=0.4811, Wilcoxon rank sum test). **(c)** The fraction of neurons not participating in any assembly was significantly higher in mutant mice (CTR: N=4 animals, n=8 (two directions for each mouse); MUT: N=5 animals, n=10 (two directions for each mouse); P=0.0434, Wilcoxon rank sum test). **(d)** Strength of assembly activation on the linear track (LT) and during the subsequent rest session was significantly lower in mutants (In LT: CTR, N=4 animals, n=118 assemblies; MUT, N=5 animals, n=119 assemblies, P (LT) = 3.196×10^{-7}; In rest session: CTR, N=4 animals, n=114 assemblies; MUT, N=5 animals, n=114 assemblies, P (rest) = 1.75×10^{-5}). All significant difference in Figure 3.2 were tested with Wilcoxon rank sum test. This figure was reproduced from (Guan et al. 2021).

To examine the bilateral participation of neurons within single assemblies and ask if assembly diversity was altered in the mutants, I compared the fraction of unilateral (containing only cells from a single hemisphere, dashed lines in **Figure 3.2 a**) and bilateral assemblies (containing cells from both hemispheres, solid lines in **Figure 3.2 a**) across the genotypes. I observed that the proportion of unilateral cell assemblies was significantly lower in control mice than in mutants, suggesting a loss of CA3 input may result in decreased bilateral assembly activity. In order to exclude the possibility that this results from an imbalance in the number of cells recorded in left and right CA1, each assembly was reconstituted 1000 times by a random draw of all cells recorded in that session and the proportion of unilateral assemblies was recalculated for each shuffle. While the fraction of shuffled unilateral assemblies was similar between

controls and mutants, only in the mutant animals was the observed fraction of unilateral assemblies significantly above this chance value (Observed CTR, 0.3587 ± 0.0199, Observed MUT, 0.5805 ± 0.0594; Shuffled CTR, 0.3014 ± 0.0148, Shuffled MUT, 0.3552 ± 0.0299; **Figure 3.3 a**). This was true across the population, as well as within single animals of both genotypes (**Figure 3.3 b**).

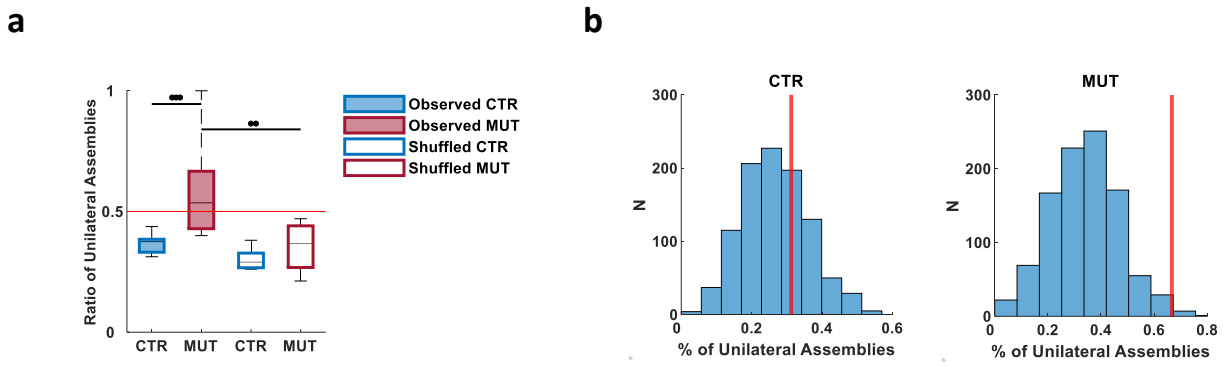

Figure 3.3 Cell assemblies were lateralized by silencing CA3 input.

(a) Fewer bilateral cell assemblies in CA3-TeTX mice. Left: the fraction of unilateral assemblies was significantly higher in mutants (CTR, N=4 animals, n=8 (two directions for each mouse); MUT, N=5 animals, n=10 (two directions for each mouse); P=0.0388, two way ANOVA, followed by post-hoc Bonferroni test, P (observed CTR *vs*. observed MUT) = 0.002, P (observed MUT *vs*. shuffled MUT) = 8.112×10^{-4}, P (observed CTR *vs*. shuffled CTR) = 1). (**b**) Examples from one control and one mutant animal demonstrate the relationship between the observed fraction of unilateral assemblies (red line) and population distribution of the shuffled reconstituted assemblies. Unless mentioned, all significant difference in Figure 3.3 were tested with Wilcoxon rank sum test. This figure was reproduced from (Guan et al. 2021).

3.3 SWRs and associated assembly reactivation are lateralized in CA3-TeTX mice.

Given that CA3 is important for the coordination of bilateral cell assembly activity across CA1, I next sought to identify how this lateralization might influence SWRs, which is characterized by the precise temporal organization of neuronal activity, both within and across hemispheres (Carr, Karlsson et al. 2012). I first compared the properties of SWRs recorded bilaterally in CA1. Consistent with the previous results in the CA3-TeTX mice (Nakashiba, Buhl et al. 2009, Middleton and McHugh 2016), I observed a decrease in the intrinsic SWRs frequency in the mutant mice, while the amplitude, occurrence and duration were

similar to controls (Frequency: CTR, 132.9 ± 5.54 HZ; MUT, 108.3 ± 2.01 HZ; Amplitude: CTR, 0.25 ± 0.020 mV; MUT, 0.22 ± 0.026 mV; Duration: CTR, 88.79 ± 5.569 ms; MUT, 81.74 ± 3.152 ms; Occurrence: CTR, 0.21 ± 0.018 / s; MUT, 0.17 ± 0.011 / s; **Figure 3.4 a**). Similar to the single cell data shown in Figure 3.1, I found no differences in any of these SWR properties between left and right CA1 in either genotype, although I did note a trend for right hemisphere SWRs to be slightly larger in amplitude and shorter in duration in the mutant mice (Frequency: CTR L, 134.1 ± 6.43 HZ, CTR R, 131.8 ± 10.04 HZ; MUT L, 105.47 ± 2.136 HZ, MUT R, 111.13 ± 3.095 HZ; Amplitude: CTR L, 0.22 ± 0.034 mV, CTR R, 0.27 ± 0.019 mV; MUT L, 0.19 ± 0.012 mV, MUT R, 0.26 ± 0.047 mV; Duration: CTR L, 87.01 ± 7.022 ms, CTR R, 90.56 ± 9.660 ms; MUT L, 82.00 ± 1.056 ms, MUT R, 81.48 ± 6.600 ms; Occurrence: CTR L, 0.21 ± 0.030 / s, CTR R, 0.21 ± 0.024 / s; MUT L, 0.16 ± 0.011 / s, MUT R, 0.18 ± 0.018 / s; **Figure 3.4 b**). However, while SWRs in the left and right hemispheres showed strong temporal coordination in control mice, the cross-correlation of SWR events in the mutants demonstrated a dramatic decrease (CTR, 3.38 ± 0.226 SWRs / s; MUT, 0.87 ± 0.063 SWRs / s; **Figure 3.4 c**), suggesting that blockade of CA3 input impaired the synchronization of bilateral CA1 population activity during rest. However, when I performed weighted phase lag index (WPLI) analysis of paired left and right CA1 LFP recordings, there was a significant increase in the WPLI following CA3 silencing in the high gamma (HG) range (WPLI 55-85Hz; CTR:0.0250 ± 0.0167; MUT:0.1215 ± 0.0605; **Figure 3.4 d**).

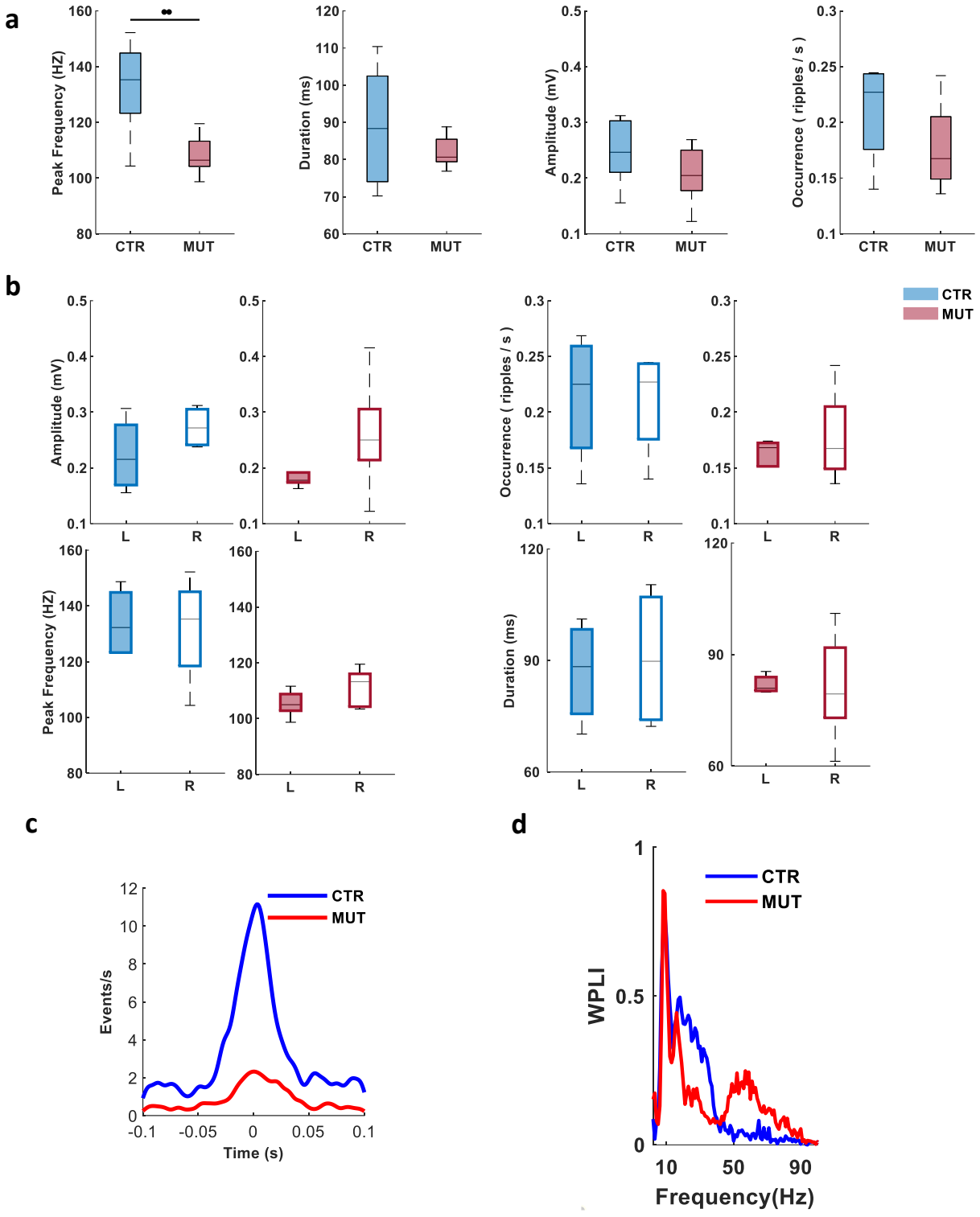

Figure 3.4 SWRs properties across genotypes and hemispheres, and gamma oscillations across hemispheres.

(**a**) Intrinsic SWRs frequency was significantly slower in mutant mice compared to controls, but amplitude, occurrence and duration were similar between genotypes (CTR, N=4 mice, n=8 tetrodes, one from each hemisphere; MUT, N=5

mice, n=10 tetrodes, one from each hemisphere; P (frequency) = 0.0021, P (amplitude) =0.2743, P (duration) = 0.5148, P (occurrence) = 0.0676). (**b**) SWRs properties were similar between left and right CA1 in both genotypes (Filled bars: left hemisphere; open bars: right hemisphere; CTR, N=4 mice, n=8 tetrodes, one from each hemisphere; MUT, N=5 mice, n=10 tetrodes, one from each hemisphere; frequency: P (CTR) = 1, P (MUT)= 0.3095; amplitude: P (CTR) = 0.4857, P (MUT) = 0.1508; duration: P (CTR) = 0.6857, P (MUT)= 0.6905; occurrence: P (CTR) = 0.8857, P (MUT) = 0.8413). (**c**) Cross-correlation of SWRs across hemispheres demonstrates a loss of temporal coordination in CA3-TeTX mice (CTR, N=4 mice, n=4 pairs of tetrodes; MUT, N=5 mice, n=5 pairs of tetrodes; P = 5.24×10^{-30}). (**d**) Group data showing WPLIs between left and right CA1 across the frequency range of 2-100 Hz (CTR, N=4 mice; MUT, N=5 mice). P (HG, coherence, 55-85 Hz) = 7.0833Hze^{-11}; CTR:0.0250 showing WPLIs between left. All significant difference in Figure 3.4 were tested with Wilcoxon rank sum test. This figure was reproduced from (Guan et al. 2021).

I next focused on the activity of cell assemblies specifically during SWRs and found rate of assembly reactivation was significantly lower in mutants than controls (CTR, 0.085 ± 0.0038 HZ; MUT, 0.067 ± 0.0041 HZ), however the overall strength of reactivation assemblies was significantly higher (CTR, 118.64 ± 20.682; MUT, 243.61 ± 32.124; **Figure 3.5 a**). I then classified single assemblies as left or right assemblies, according to which hemisphere contributed the majority of units. I compared the reactivation of left assemblies with right assemblies during right hemisphere SWRs. In control mice, reactivation was similar between left and right assemblies (Strength: L = 91.10 ± 8.425, R = 178.35 ± 65.182; rate: L = 0.082 ± 0.0046 HZ, R = 0.084 ± 0.0082 HZ; **Figure 3.5 b**), however in the mutant mice the reactivation rate was significantly higher during SWRs detected in the same (right) hemisphere that dominated the assembly (right assemblies) (Strength: L = 304.58 ± 58.467, R = 204.00 ± 41.284; rate: L = 0.052 ± 0.0048 HZ, R = 0.074 ± 0.0069 HZ; **Figure 3.5 c**).

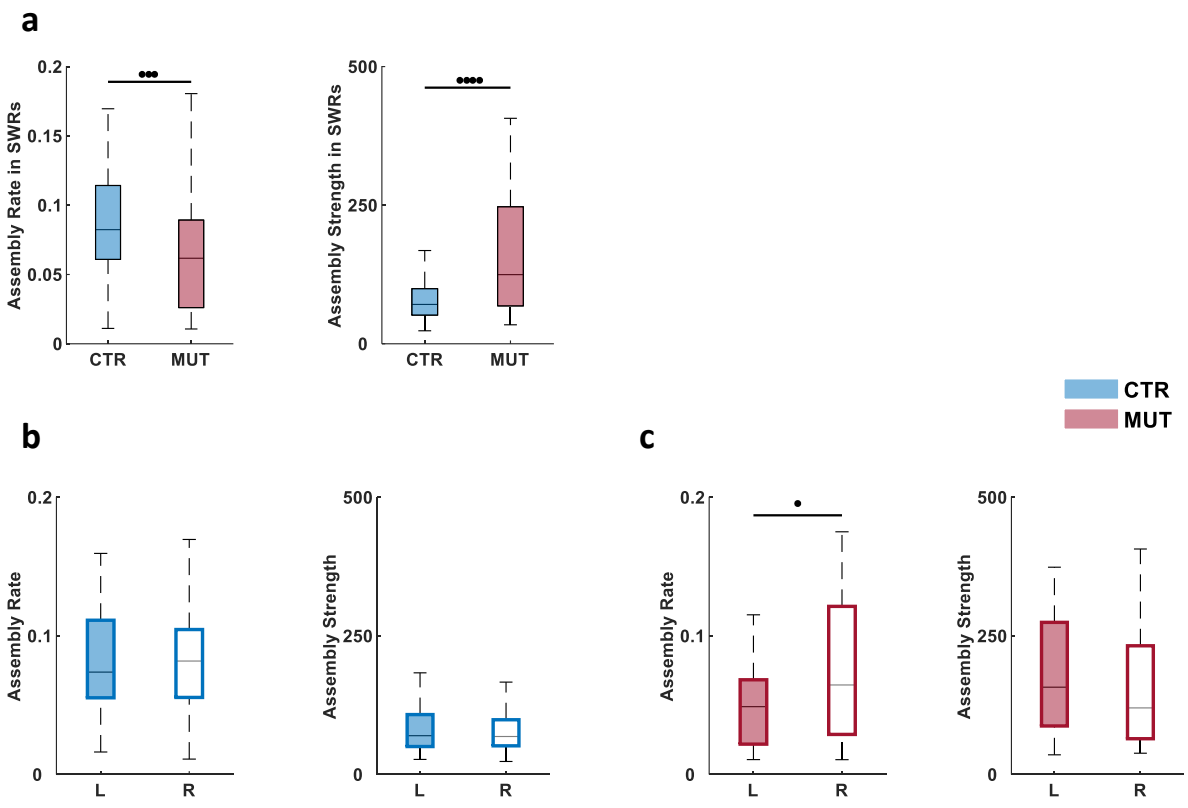

Figure 3.5 CA3 input is required for bilateral coordination of assembly reactivation.

(**a**) Assembly reactivation rate during SWRs was significantly reduced in mutants (CTR, N = 4 mice, n = 115 assemblies; MUT, N=5 mice, n=118 assemblies; $P = 1.27 \times 10^{-7}$), however strength was significantly increased ($P=2.81 \times 10^{-4}$, Wilcoxon rank sum test). (**b**) The reactivation of strength and rate of right assemblies and left assemblies were similar in control (CTR, N=4 mice, n (right assemblies with right ripple) = 35, n (left assemblies with right ripple) = 61, P (strength) = 0.0836, P (rate) = 0.7678). (**c**) Right assembly reactivate faster than left assembly during right ripple in MUT, but strength remained similar (MUT, N=5 mice, n (right assemblies with right ripple) = 46, n (left assemblies with right ripple) = 53, P (strength) = 0.1707, P (rate) = 0.0388). Unless mentioned, all significant difference in Figure 3.5 were tested with LMMs. This figure was reproduced from (Guan et al. 2021).

3.4 CA3 input is required for replay sequences across bilateral CA1.

Previous research has shown that the temporally coordinated SWR-associated replay of sequences of place cells observed during behavior is coordinated across hemispheres (Carr, Karlsson et al. 2012). Given that the silencing of CA3 input decreased not only the synchronization of bilateral SWRs, but also the co-activation of bilateral CA1 cell assemblies during rest, I asked whether CA3 input is critical for the coordination of bilateral CA1 neurons in replay sequences. I first used the combined activity of CA1

pyramidal cells recorded bilaterally during SWRs period to identify significant replay event sequences (**Figure 3.6 a**). Despite the loss of CA3 transmission, replay was observed in the mutant mice, however the quality of these significant replay events was significantly worse (Z score of weighted correlation: CTR, 2.25 ± 0.028; MUT, 2.12 ± 0.026; **Figure 3.6 b**). Further, compared to controls, on average the replay events in the mutants were faster in decoded speed (CTR, 6.64 ± 0.186 m/s; MUT, 7.44 ± 0.213 m/s; **Figure 3.6 b**), covered larger distances (CTR, 78.53 ± 1.753 cm; MUT, 83.04 ± 2.060 cm; **Figure 3.6 b**) and exhibited larger mean jump distances between adjacent decoded positions in mutant mice (CTR, 15.06 ± 0.353 cm; MUT, 17.37 ± 0.438 cm; **Figure 3.6 b**).

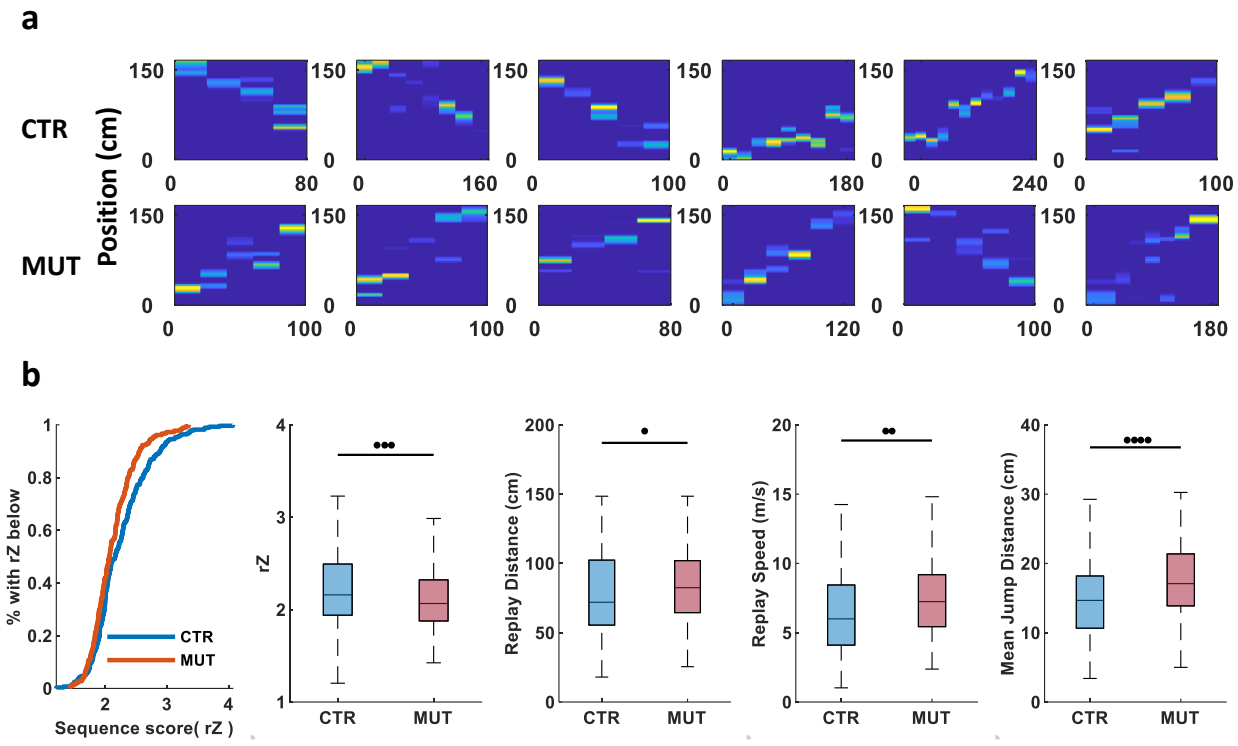

Figure 3.6 CA3 input is required for bilateral replay sequences in CA1.

(a) Examples of trajectory sequences derived from Bayesian decoding of spiking activity from bilateral CA1 during SWRs periods. Top: controls; bottom: mutants. Colors are scaled to posterior probability of each significant decoded replay event in 20 ms time bins (blue, minimum; yellow, maximum). **(b)** The quality of significant replay events decoded with cells from bilateral CA1 during SWRs detected in either hemispheres was reduced in mutant mice (left: population distribution, right: box plot), however replay distance, speed and mean jump distance between adjacent positions were higher (CTR: N = 4 animals, n (right ripple) = 166 events , n (left ripple) = 111 events, n (combined) = 277 events; MUT: N = 5 animals, n (right ripple) = 103 events, n (left ripple) =79 events, n (combined) =182 events; P (rZ) = 0.0037, P (replay speed) = 0.0012, P (replay distance) =

0.0408, P (mean jump distance) = 1.1602×10^{-5}). All significant difference in Figure 3.6 were tested with Wilcoxon rank sum test. This figure was reproduced from (Guan et al. 2021).

Finally, the presence of replay events in both genotypes allowed me to compare the contribution of left and right CA1 cells to each replay event and assess their lateralization. I focused on significant replay events decoded using bilaterally recorded neurons that were detected during SWRs recorded in the same or opposite hemisphere and determined each place cell's contribution to the sequence by calculating the Per Cell Contribution (PCC) score averaged across all significant events (Grosmark and Buzsaki 2016). In control mice, CA1 neurons demonstrated similar contribution to replays occurring during SWRs in the same and opposite hemispheres (CTR same, 4.86 ± 0.244; CTR opposite, 5.33 ± 0.294), however in mutant mice the PCC scores of cells during ripples from same hemisphere were significantly higher than those from opposite hemisphere (MUT same, 5.76 ± 0.335; MUT opposite, 4.57 ± 0.272; **Figure 3.7 a**), suggesting that silencing CA3 weakens coordinated memory replay across bilateral CA1. To examine this directly I decoded place cell spikes from a single hemisphere during SWRs detected either in the same (ipsilateral) or opposite (contralateral) hemisphere. Once more, in control mice the replay quality was similar in the same and opposite groups, however in the CA3-TeTX mice replay quality was significantly lower when only neurons from the opposite hemisphere were used (CTR same, 2.13 ± 0.028; CTR opposite, 2.12 ± 0.028; MUT same, 2.17 ± 0.029; MUT opposite, 2.10 ± 0.026; **Figure 3.7 b**).

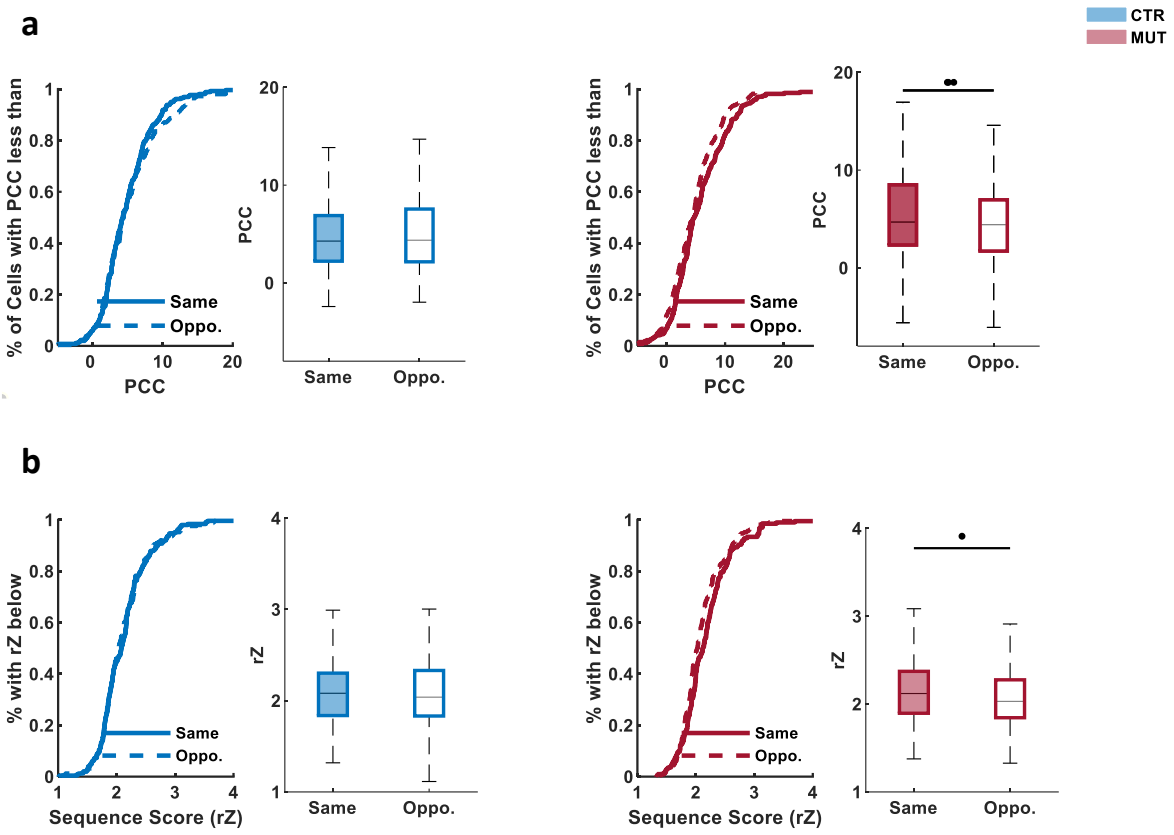

Figure 3.7 CA3 input is required for bilateral coordination replay sequences in CA1.

(a) Per cell contribution of single neuron to replay events during SWRs from the same and opposite hemispheres was similar in control mice, but in mutants neurons from the same hemisphere with ripple had significantly higher contribution (CTR, N = 4 mice, n (left cell + left ripple) = 145, n (right cell + left ripple) = 116, n (left cell + right ripple) = 139, n (right cell + right ripple) = 115, n (same hemisphere) = 260, n (opposite hemispheres) = 255, P = 0.5167; MUT, N=5 mice, n (left cell + left ripple) = 155, n (right cell + left ripple) = 148, n (left cell + right ripple) = 118, n (right cell + right ripple) = 117, n (same hemisphere) = 267, n (opposite hemispheres) = 271, P = 0.0061) **(b)** Significant replay events decoded with cells from a single hemisphere during SWRs detected in the same or opposite hemisphere were of similar quality in control mice, while in mutants replay quality was significantly lower when only contralateral neurons were used (CTR: N = 4 animals, n (left cells + left ripple) = 136 events, n (right cells + right ripple) = 112 events, n (same hemisphere in total) = 248 events; n (left cells + right ripple) = 186 events, n (right cells + left ripple) = 65 events, n (opposite hemisphere in total) = 251 events, P = 0.8796; MUT: N=5 animals, n (left cells + left ripple) = 99 events, n (right cells + right ripple) = 116 events, n (same hemisphere in total) = 196 events; n (left cells + right ripple) = 127 events, n (right cells + left ripple) = 80 events, n (opposite hemisphere in total) = 207 events, P = 0.0346). All significant difference in Figure 3.7 were tested with LMMs. This figure was reproduced from (Guan et al. 2021).

4 Discussion

4.1 Overall discussion

By exploiting the ability to chronically silence CA3 transmission I demonstrated that CA3 activity plays a key role in the bilateral coordination of CA1 spatial coding, both during behavior and periods of consolidation. I observed that while cell assembly activity, SWRs and replay all endure following the chronic silencing of CA3, their properties are altered, becoming poorer in quality and more lateralized. Interestingly, the replay trajectories in the mutant mice were faster, longer and exhibited greater jump distances, consistent with the inability of the CA3 recurrent attractor network to contribute to their structure (Pfeiffer and Foster 2015). Moreover, I observed a loss of temporal coordination between SWR events across the left and right hemispheres, leading to an impairment and lateralization in the re-expression of bilateral sequences of place cell activity following exploration.

The phenotypes observed in the CA3-TeTX mice are distinct from those seen in experiments using optogenetics to transiently silence the CA3 axon terminals, which resulted in a decrease in the occurrence of SWRs in addition to poorer replay quality across CA1 (Yamamoto and Tonegawa 2017, Davoudi and Foster 2019). In contrast to the fast transient local inhibition provided by optogenetics, the transgenic approach allows me to induce the silencing of CA3 in adult mice just prior to recording in a comparatively slow manner. Thus, there may be compensation due to the chronic nature of the manipulation which allows SWRs and temporal spike coding, albeit with altered properties, to persist, even in a more lateralized manner. Despite this, it is important to note that the transgenic mice permit silencing of transmission across all CA3 pyramidal cells (Nakashiba, Young et al. 2008), providing a more complete and reproducible model to study these phenomena and answer the question of exactly what CA3 input contributes. I believe that the complementary nature of acute and chronic approaches has established that both are critical for understanding the importance of this circuit and its role in memory.

4.2 The importance of bilateral CA1 recording in mice.

As the hippocampus is thought to be crucial for memory formation, consolidation and retrieval, previous research has focused on the mechanism of these memory processes across the hippocampal circuit. In many of these studies neural activity was recorded from the different subregions of the hippocampus while the animal was freely moving in various tasks related to episodic memory. However, most of the published research presented results and conclusions under unilateral hippocampal recording, mostly on the right side, as it was widely thought that there is no lateralization in the brain of rodents. While the lateralization of function within the human hippocampus has been clearly demonstrated (Burgess, Maguire et al. 2002, Maguire and Frith 2003), very few studies have focused on the lateralization of rodent hippocampus, and of those that have addressed the question, they have provided mixed evidence. Lateralization of anatomical connectivity, spine size and capacity for synaptic plasticity have been noted in the mouse hippocampus, mainly focusing on the CA3 to CA1 circuits (Kawakami, Shinohara et al. 2003, Jordan 2020). Further, previous *in vivo* physiological studies focused on hippocampal lateralization have noted differences in both the synchronization of gamma and ripple oscillations and functions between the hemispheres (Benito, Martín-Vázquez et al. 2016, Villalobos, Maldonado et al. 2017, Song, Wang et al. 2020), including a differential contributions of left and right CA3 during the retrieval of spatial working memory (Song, Wang et al. 2020). In fiber photometry recording of bilateral CA3 activity in mice performing a spatial working memory T-maze task, neurons in left CA3 showed more activity than right CA3 specifically during the choice phase. In addition, performance was impaired only when neurons in left CA3 were silenced optogenetically (Song, Wang et al. 2020). In another study, gamma oscillations recorded from bilateral CA3 under anesthesia were found to be asymmetric and lateralized, with higher amplitude in the right hemisphere (Benito, Martín-Vázquez et al. 2016). The synchronization of gamma oscillation from bilateral CA1 was disrupted by blocking the interhemispheric connection between bilateral CA3, suggesting that the left and right sides of hippocampus do not transfer the same information (Benito, Martín-Vázquez et al. 2016). Villalobos et al. performed local-field potential recording from bilateral CA1 in rats during slow-wave sleep and reported that ripple oscillations from left and right hippocampi are asynchronous

(Villalobos, Maldonado et al. 2017). Here I observed a much higher degree of temporal synchrony of L/R ripple in the control mice, consistent with earlier studies in rats (Suzuki and Smith 1987), suggesting that differences in species, strain or analysis method may underlie these divergent results. Despite the lateralization reported on the level of synchronization of gamma and ripple oscillations, the interhemipsheric integration of spatial representations during exploration and rest has been repeatedly observed (Carr, Karlsson et al. 2012, Pfeiffer and Foster 2013), suggesting integration of the hippocampal spatial code. My results support this conclusion, as I observed no lateralization between the left and right sides of hippocampus on both the single cell and ensemble levels in control mice, however the increase in lateralization in the CA3-TeTX animals suggests that the CA3 to CA1 projections may be responsible for this function.

4.3 Cell assemblies and replay

4.3.1 Increased strength of cell assemblies during SWRs following CA3 inhibition

In Figure 3.5a, I showed that the rate of cell assembly activation during SWRs was significantly lower in mutants than in controls, surprisingly however, the strength was significantly higher. The higher assembly strength in mutant might be a consequence of chronic silencing of CA3. The blockage of CA3 with TeTX is a method that has a relative slow kinetics and as a result, the silencing of CA3 might lead to an increase in neural activity in the bilateral CA1. The increased co-activation of CA1 pyramidal cells is consistent with the data shown in earlier experiments on these mice (Nakashiba, Buhl et al. 2009), which suggests that silencing CA3 through TeTX, may result in higher firing rates in CA1 pyramidal cells, although below the level of significance; perhaps due to similar increases in local feedback inhibition. Thus, the increased strength of CA1 cell assembly co-activation I observed could be interpreted as a compensation of CA3 blockage. In addition, this result is also consistent with the higher gamma band (55-85 Hz) coherence between bilateral CA1 in the mutants observed in this study (**Figure 3.4 d**).

It is also important to note that the silencing of CA3 output might also decrease the feedforward excitation of inhibitory neurons in the local circuit of CA3, leading to an activation of neural activity in CA1 which receives input from a subset of CA1-projecting inhibitory neurons in CA3.

4.3.2 Preserved replay

In terms of the circuitry underlying replay, hitherto it had been impossible to record the reactivation of place cell trajectories during SWRs in CA3-TeTX mice due to the technical challenges in recording a sufficient number of neurons simultaneously in mouse. Here, the high-density bilateral tetrode recording permitted this analysis for the first time and I found, contrary to expectation, that even with CA3 transmission completely silenced, replay does persist, albeit with some alterations and, importantly, in a more lateralized manner.

The blockade of CA3 by genetic tools did not disrupt the replay of bilateral CA1, however it did decrease the quality of significant replay events, suggesting that CA3 might not be the sole origin of CA1 replay. Although it is widely accepted that CA3 is the primary driver of SWRs and replay events, there is evidence that SWRs can be triggered by other inputs, including those from CA2 (Oliva, Fernandez-Ruiz et al. 2016, Oliva, Fernandez-Ruiz et al. 2020), the subiculum (Imbrosci, Nitzan et al. 2021) and perhaps also intrinsically generated within CA1 itself (Maier, Nimmrich et al. 2003). Moreover, recent *in vivo* evidence has established that activity in CA2 contributes to both SWR generation and reactivation of cell assemblies, even when CA3 is intact (Oliva, Fernandez-Ruiz et al. 2016, Oliva, Fernandez-Ruiz et al. 2020). Single-unit recordings from all CA subregions demonstrate that prior to the characteristic bursting observed in CA3, which has been taken as a signal for the onset of SWRs, CA2 pyramidal cell population can display a biphasic activity pattern preceding its neighbors (Oliva, Fernandez-Ruiz et al. 2016). This activity is then successively evident in areas CA3a, CA3b, CA3c, and finally CA1 with brief temporal delays. Moreover, Oliva et al. further demonstrated structured reactivation of socially active neurons during these CA2 SWR events, manipulation to which could impact memory (Oliva, Fernandez-Ruiz et al. 2020). Further, a very recent study provided both *in vitro* and *in vivo* evidence that the subiculum can serve as a secondary

independent SWR generator, leading to events that propagate backwards into CA1 (Imbrosci, Nitzan et al. 2021). Although that study did not examine replay, it raises the possibility that SWRs seen in the absence of CA3 transmission may also have a subicular origin. Finally, there is evidence from *in vitro* studies that CA1 can generate SWRs by itself, when all other hippocampal subfields are dissected away (Maier, Nimmrich et al. 2003). Although it is not possible to distinguish these possibilities from the current study, given that CA3 primarily acts to inhibit CA2 *in vivo* (Boehringer, Polygalov et al. 2017), and even under normal conditions CA2 is responsible for generating a proportion of normal SWRs in CA1, my belief is that CA2 most likely acts to initiate SWRs in the absence of CA3 output; hopefully this can be experimentally tested in future studies.

In this study the number of SWRs and significant replay events remained similar following blockade of CA3 input, which offered an opportunity to identify the differential roles of bilateral CA1 in replay. However I did observed that the quality of replay was worse in mutants. Interestingly, the replay trajectories in the mutant mice were faster and longer and exhibited greater jump distances, which is consistent with the phenomenon of replay properties that were observed with the inability of the CA3 recurrent attractor network (Pfeiffer and Foster 2015). This result is also consistent with the increase in replay speed during light on in Supplementary Figure 11 from the Davoudi and Foster study (Davoudi and Foster 2019). In that experiment, recording were performed in both control and experimental rats with 20s laser on and 20s laser off in each session, which experimental rats expressing the light-activated proton pump eArch3.0 in bilateral CA3.

4.3.3 Cell assemblies vs. Replay

It has been suggested that memory of events that animal experiences is stored across a wide population of neurons, rather than in single cells (Wilson and McNaughton 1993). According to this, after an experience, the synaptic and functional connections among place cells in hippocampus become altered. It has also been suggested that the co-activation of groups of CA1 cells with overlapping place fields are selectively facilitated in the sleep session right after exploration tasks (Dupret, O'Neill et al. 2010). However,

while this facilitated co-activation of place cells with overlapping place fields suggests experience-dependent changes in activity, it does not mean the existence of longer sequences of ensemble activity that may govern episodic memory in hippocampus (Tulving 2002). Rather, the replay of sequences of place cell activity in the sleep session after exploration that reflects the activation order of the cells during previous movement on linear tracks (Skaggs and McNaughton 1996, Lee and Wilson 2002, Davidson, Kloosterman et al. 2009, Karlsson and Frank 2009) is widely thought to represent the property of cell ensembles in CA1 for learning and memory consolidation. Furthermore, it was suggested that the replay can be explained by the repeated activation of cell assemblies in hippocampus. Crucially, unlike during behavior whereby neurons are activated over tens of seconds or minutes, during replay the same cell assemblies reactivate over much shorter periods, typically 100 ms or so, which promotes synaptic plasticity and results in the strengthening of the cell assemblies (Farooq, Sibille et al. 2019).

4.4 Behavioral impact related to increased lateralization by silencing CA3

While earlier behavioral characterization of the CA3-TeTX mice identified learning deficits in novel environments, suggesting that CA3 output plays an important role in rapidly forming representation of a novel context (Nakashiba, Young et al. 2008), as well as in pattern completion-based recall (Nakashiba, Young et al. 2008), the mutant mice performed normally during training and recall in the Morris water maze (Nakashiba, Young et al. 2008). It has been suggested that left and right CA3 may play different roles during the acquisition and retrieval of a spatial memory, with left CA3 more responsible for the storage of discrete locations within an environment and discrimination of distinct places during retrieval, and right CA3 more responsible for the integration of route information in spatial working memory tasks (Jordan 2020). In the research using CA3-TeTX mice, although there was increased lateralization by silencing CA3 input, the intact learning in water maze does not directly support this hypothesis. This might be explained by the limitation of the CA3-TeTX mouse model, as it is not possible to disambiguate the role of bilateral CA3 to CA1 projections from that of contralateral CA3 to CA3 projections in the lateralization observed here. Future work with more spatially targeted approaches may be necessary, for example, experiments

designed to inhibit the terminal of CA3 input in CA1 only or selectively inhibiting left or right CA3 projections.

Since the poorer quality and more lateralized cell assemblies and replays observed following the blockade of CA3-CA1 transmission were all recorded when the animals were navigating in a familiar environment, I expect that these effects will be stronger if neural activity was recorded in a novel context, as Nakashiba et al. showed a learning deficit in novel environment(Nakashiba, Young et al. 2008) . In this study I chose to record in a familiar environment to simplify my interpretation of the reactivation data.

4.5 Advantages and limitation of this study

4.5.1 Advantages and limitation of CA3-TeTX transgenic mice

The genetic approach taken in this study allowed me to induce the silencing of CA3 in adult mice just prior to recording, without virus injection and expression, avoiding the risk of low or even no expression of viral genes in the target area. As I can only check the expression of virus after recording with an implantation of micro-drive, these experiments are less efficient than those using transgenic mice. Furthermore, the effect of silencing with transgenic mice is more complete, as it is difficult for an injected virus to be expressed in all cells of the anatomically distributed targeted area. Further, in addition to the anatomical restrictions of viral injection, it is also hard to ensure that expression in all cells is at the same level. In addition, an optic fiber is implanted into the brain area for delivering light in optogenetic experiments and the size of optic fiber is big compared with the size of mice brain, risking damage to brain tissue. With the transgenic mice, the activity of cells is manipulated simply by changing the diet of the animals. The ability to activate or inhibit the activity of a population of neurons at millisecond time scales has led to the popularity of optogenetics, however, optogenetic stimulation can cause an abnormal condition of neurons, which may have opposite and unexpected consequences. For example, a strong and long exposure of laser for inhibiting neural activity may lead to a non-physiological hyperpolarization, which

can cause rebound excitation even though there is releasing of inhibitory process (Kravitz and Bonci 2013, Häusser 2014).

Although there are several advantages in using transgenic mice, the kinetics are relatively slow, thus there may be compensation due to the chronic nature of the manipulation which allow SWRs and temporal coding to persist or even increase. Also, the circuit manipulation in transgenic mice is less flexible than optogenetics, as it is not possible to inactivate neural activity in bilateral hippocampus separately with the genetic method, which is easy when using optogenetics.

4.5.2 Limitation of using only male mice in this study

It has been suggested by many that the consideration of sex as a biological variable is crucial for the future of neuroscience (Shansky 2019). It is important to note that a limitation of the CA3-TeTX model to date is that the kinetics and efficacy of the transgenic blockade of transmission has only been verified in male mice (Nakashiba, Young et al. 2008), thus in this study female mice were not included. Previous work has noted no sex differences in hippocampal lateralization (Jordan, Shanley et al. 2019), however future work should address the role of CA3 transmission in the integration of the CA1 spatial code in female mice.

4.6 Future directions

4.6.1 Dissociation of CA3-ipsilateral CA1 and CA3-contralteral CA1 projections

In the mouse model I used in my study the projections from bilateral CA3 into left and right CA1 are both blocked, thus it is not possible to tell if there are functional difference between the circuits of CA3 projections to ipsilateral and contralateral CA1. In order to dissociate the two circuits, optogenetics are required to silence the terminals of single hemispherical CA3 fibers to either ipsilateral CA1 or contralateral CA1 separately, allowing a comparison of activity of bilateral CA1 neurons. I am planning to combine CA3-Cre transgenic mice, which has Cre recombinase expression in bilateral hippocampal CA3, with the AAV-EF1a-DIO-eArchT3.0-EYFP vector, which is a virus containing a light sensitive protein, injected into either left or right side of CA3. Then yellow-green laser with the wave length of 561 nm applied on

the terminal of CA3 input in the stratum oriens of left or right CA1would specifically silence ipsi or contralateral projections during the simultaneous recording of activity from bilateral CA1. In order to avoid the rebound effect mentioned above, virus expression and the power and duration of light delivery should be carefully controlled.

4.6.2 Functional dissociation of left and right CA3.

It was reported that there are differences in anatomy, molecular components, synaptic plasticity, and behavior in CA3-CA1 synapses, relating to the hemispheric origin of CA3 input(Kawakami, Shinohara et al. 2003, Shinohara, Hirase et al. 2008, Kohl, Shipton et al. 2011, Shipton, El-Gaby et al. 2014, Jordan 2020, Song, Wang et al. 2020). For example, small, GluN2B-rich spines in bilateral CA1 mainly received input from left CA3, however large GluA1-rich spines in bilateral CA1 mainly received input from right CA3. It is also suggested, GluA1 at CA1 synapses receiving right CA3 input is more than the ones at CA1 synapses receiving input from left CA3(Shinohara, Hirase et al. 2008). Furthermore, it has been shown that only the synapses receiving input from left CA3 could generate long term potentiation (Shipton, El-Gaby et al. 2014). Fiber photometry recording of bilateral CA3 activity in mice performing a spatial working memory T-maze task revealed that neurons in left CA3 showed more activity than right CA3 specifically during the choice phase. In addition, performance was impaired only when neurons in left CA3 were silenced using optogenetics (Song, Wang et al. 2020).

Based on the studies above, I will apply the same experimental method as described in 4.6.1, which combines CA3-Cre transgenic mice with AAV-EF1a-DIO-eArchT3.0-EYFP. Yellow-green laser with the length of 561 nm will also be given with a pulse of 20 s laser on and 20 s laser off on the terminal of CA3 input in the stratum oriens of the both CA1. The same set of analyses including single cell properties, SWRs, cell assembly, replay and so on will be applied to compare the functions of left CA3 with right CA3 input. The hypothesis will be silencing right CA3 has a smaller effect on CA1 lateralization than silencing left CA3, according to the previous studies in anatomical difference and behavior.

4.6.3 Effect of simultaneously silencing CA3 and CA2 on neural activity in bilateral CA1

The results in this study suggest that silencing CA3 cannot totally disrupt SWRs and replay of the bilateral CA1 activity, although there was a significant decrease in the quality of cell assemblies and replay trajectories which was more lateralized. Furthermore, given that CA3 primarily acts to inhibit CA2 in vivo (Boehringer, Polygalov et al. 2017) and under normal conditions CA2 is responsible for generating a proportion of normal SWRs in CA1, my belief is that CA2 most likely acts to initiate SWRs in the absence of CA3 output. According to the discussion on the origin of SWRs and replay in 4.3, it is reasonable to predict that when silencing both CA3 and CA2 at the same time, cell ensembles in bilateral CA1 will be disrupted, including SWRs and replay events. In my future plans, CA3-TeTX mice will be crossed with CA2-Cre mice, which makes it possible to block CA3 as well as to silence CA2 by injecting Cre-dependent virus in bilateral CA2.

5 Conclusion

In conclusion, by exploiting the ability to chronically silence CA3 transmission I demonstrate that these projections play a key role in the cross-hemispheric coordination of CA1 spatial coding, during both behavior and periods of consolidation. These results help explain the gap between the works demonstrating lateralization in the rodent hippocampus at the in vitro level (Kohl, Shipton et al. 2011, Shipton, El-Gaby et al. 2014) and bilateral place cell recordings which failed to find strong hemispheric differences (Carr, Karlsson et al. 2012, Pfeiffer and Foster 2013). Further, I observed that cell assemblies, SWRs and replay endured following the chronic silencing of CA3 transmission, however the properties of ensemble events were significantly altered, not only becoming poorer in quality, but also more lateralized. This is consistent with a previous work using optogenetics to transiently silence the CA3 axon terminals, which degraded the replay quality in bilateral CA1 (Davoudi and Foster 2019). Interestingly, the replay trajectories in the mutant mice were faster and longer and exhibited greater jump distances, consistent with the inability of the CA3 recurrent attractor network to contribute to their structure (Pfeiffer and Foster 2015). Moreover, I observed a loss of temporal coordination between SWR events across the left and right hemispheres, leading to an impairment and lateralization in the re-expression of bilateral sequences of place cell activity following exploration. I found no significant differences in any of these SWR properties between left and right CA1 in either genotype, however I did note a trend for right hemisphere SWRs to be slightly larger in amplitude and shorter in duration in the mutant mice, which suggested that there might be lateralization in SWRs in rodent, but the difference was much weaker than that in human beings.

Although the genetic approach allowed me to induce the silencing of CA3 in adult mice just prior to recording, the time course of silencing was relatively slow, as it took four weeks for the completely inhibition of CA3 output, thus compensations might hve happened, albeit with altered properties and temporal coding were observed. Further I could not disambiguate the role of bilateral CA3 to CA1 projections from that of contralateral CA3 to CA3 projections in the context of lateralization observed here. Future work with more spatially targeted approaches may be necessary. Nonetheless, these findings provide

the first in vivo evidence of the importance of CA3 transmission in the maintenance of neural ensemble coordination between left and right CA1.

6 Reference List

Alme, C. B., C. Miao, K. Jezek, A. Treves, E. I. Moser and M.-B. Moser (2014). "Place cells in the hippocampus: Eleven maps for eleven rooms." Proc Natl Acad Sci USA **111**(52): 18428-18435.

Andersen, P., R. Morris, D. Amaral, T. Bliss and J. O'Keefe (2006). The Hippocampus Book, Oxford University Press, USA.

Benito, N., G. Martín-Vázquez, J. Makarova, V. A. Makarov and O. Herreras (2016). "The right hippocampus leads the bilateral integration of gamma-parsed lateralized information." eLife **5**:e16658.

Boehringer, R., D. Polygalov, A. J. Y. Huang, S. J. Middleton, V. Robert, M. E. Wintzer, R. A. Piskorowski, V. Chevaleyre and T. J. McHugh (2017). "Chronic Loss of CA2 Transmission Leads to Hippocampal Hyperexcitability." Neuron **94**(3): 642-655 e649.

Bostock, E., R. U. Muller and J. L. Kubie (1991). "Experience-dependent modifications of hippocampal place cell firing." Hippocampus **1**(2): 193-205.

Buhl, D. L., K. D. Harris, S. G. Hormuzdi, H. Monyer and G. Buzsaki (2003). "Selective impairment of hippocampal gamma oscillations in connexin-36 knock-out mouse in vivo." J Neurosci **23**(3): 1013-1018.

Burgess, N., E. A. Maguire and J. O'Keefe (2002). "The human hippocampus and spatial and episodic memory." Neuron **35**(4): 625-641.

Buzsaki, G. (1986). "Hippocampal sharp waves: their origin and significance." Brain Res **398**(2): 242-252.

Buzsaki, G. (1989). "Two-stage model of memory trace formation: a role for "noisy" brain states." Neuroscience **31**(3): 551-570.

Buzsaki, G. (2005). "Theta rhythm of navigation: link between path integration and landmark navigation, episodic and semantic memory." Hippocampus **15**(7): 827-840.

Buzsaki, G. (2015). "Hippocampal sharp wave-ripple: A cognitive biomarker for episodic memory and planning." Hippocampus **25**(10): 1073-1188.

Buzsáki, G., Z. Horváth, R. Urioste, J. Hetke and K. Wise (1992). "High-frequency network oscillation in the hippocampus." Science **256**: 1025-1027.

Cacucci, F., T. J. Wills, C. Lever, K. P. Giese and J. O'Keefe (2007). "Experience-dependent increase in CA1 place cell spatial information, but not spatial reproducibility, is dependent on the autophosphorylation of the alpha-isoform of the calcium/calmodulin-dependent protein kinase II." J Neurosci **27**(29): 7854-7859.

Carr, M. F., S. P. Jadhav and L. M. Frank (2011). "Hippocampal replay in the awake state: a potential substrate for memory consolidation and retrieval." Nat Neurosci **14**(2): 147-153.

Carr, M. F., M. P. Karlsson and L. M. Frank (2012). "Transient slow gamma synchrony underlies hippocampal memory replay." Neuron **75**(4): 700-713.

Cembrowski, M. S. and N. Spruston (2019). "Heterogeneity within classical cell types is the rule: lessons from hippocampal pyramidal neurons." Nat Rev Neurosci **20**(4): 193-204.

Collingridge, G. L., S. J. Kehl and H. McLennon (1983). "Excitatory amino acids in synaptic transmission in the schaffer collateral-commissural pathway of the rat hippocampus." J Physiol (Lond) **334**: 33-46.

Concha, M. L., I. H. Bianco and S. W. Wilson (2012). "Encoding asymmetry within neural circuits." Nat Rev Neurosci **13**(12): 832-843.

Corballis, M. C. (2012). "Lateralization of the human brain." Prog Brain Res **195**: 103-121.

Csicsvari, J., B. Jamieson, K. D. Wise and G. Buzsáki (2003). "Mechanisms of gamma oscillations in the hippocampus of the behaving rat." Neuron **37**(2): 311-322.

Danjo, T. (2020). "Allocentric representations of space in the hippocampus." Neurosci Res **153**: 1-7.

Danjo, T., T. Toyoizumi and S. Fujisawa (2018). "Spatial representations of self and other in the hippocampus." Science **359**(6372): 213-218.

Davidson, T. J., F. Kloosterman and M. A. Wilson (2009). "Hippocampal replay of extended experience." Neuron **63**(4): 497-507.

Davoudi, H. and D. J. Foster (2019). "Acute silencing of hippocampal CA3 reveals a dominant role in place field responses." Nat Neurosci **22**(3): 337-342.

Derdikman, D. and M. B. Moser (2010). "A dual role for hippocampal replay." Neuron **65**(5): 582-584.

Diba, K. and G. Buzsáki (2007). "Forward and reverse hippocampal place-cell sequences during ripples." Nat Neurosci **10**(10): 1241-1242.

Dragoi, G. and G. Buzsaki (2006). "Temporal encoding of place sequences by hippocampal cell assemblies." Neuron **50**(1): 145-157.

Dragoi, G. and S. Tonegawa (2011). "Preplay of future place cell sequences by hippocampal cellular assemblies." Nature **469**(7330): 397-401.

Dupret, D., J. O'Neill, B. Pleydell-Bouverie and J. Csicsvari (2010). "The reorganization and reactivation of hippocampal maps predict spatial memory performance." Nat Neurosci **13**(8): 995-1002.

Ego-Stengel, V. and M. A. Wilson (2010). "Disruption of ripple-associated hippocampal activity during rest impairs spatial learning in the rat." Hippocampus **20**(1): 1-10.

Eichenbaum, H., C. Stewart and R. G. M. Morris (1990). "Hippocampal representation in place learning." J Neurosci **10**(11): 3531-3542.

El-Gaby, M., Y. Zhang, K. Wolf, C. J. Schwiening, O. Paulsen and O. A. Shipton (2016). "Archaerhodopsin Selectively and Reversibly Silences Synaptic Transmission through Altered pH." Cell Rep **16**(8): 2259-2268.

Etienne, A. S. and K. J. Jeffery (2004). "Path integration in mammals." Hippocampus **14**(2): 180-192.

Farooq, U., J. Sibille, K. Liu and G. Dragoi (2019). "Strengthened Temporal Coordination within Pre-existing Sequential Cell Assemblies Supports Trajectory Replay." Neuron **103**(4): 719-733.

Finnerty, G. T. and J. G. Jefferys (1993). "Functional connectivity from CA3 to the ipsilateral and contralateral CA1 in the rat dorsal hippocampus." Neuroscience **56**(1): 101-108.

Foster, D. J. and M. A. Wilson (2006). "Reverse replay of behavioural sequences in hippocampal place cells during the awake state." Nature **440**(7084): 680-683.

Foster, D. J. and M. A. Wilson (2007). "Hippocampal theta sequences." Hippocampus **17**(11): 1093-1099.

Girardeau, G., K. Benchenane, S. I. Wiener, G. Buzsaki and M. B. Zugaro (2009). "Selective suppression of hippocampal ripples impairs spatial memory." Nat Neurosci **12**(10): 1222-1223.

Grosmark, A. D. and G. Buzsaki (2016). "Diversity in neural firing dynamics supports both rigid and learned hippocampal sequences." Science **351**(6280): 1440-1443.

Guan, H., S. J. Middleton, T. Inoue and T. J. McHugh (2021) "Lateralization of CA1 assemblies in the absence of CA3 input." Nat Commun (in press).

Hartley, T., C. Lever, N. Burgess and J. O'Keefe (2014). "Space in the brain: how the hippocampal formation supports spatial cognition." Philos Trans R Soc Lond B Biol Sci **369**(1635): 20120510.

Häusser, M. (2014). "Optogenetics: the age of light." Nat Methods **11**(10): 1012-1014.

Hebb, D. O. (1949). The Organization of Behavior: A Neuropsychological Theory. New York, John Wiley & Sons.

Hirase, H., X. Leinekugel, A. Czurko, J. Csicsvari and G. Buzsaki (2001). "Firing rates of hippocampal neurons are preserved during subsequent sleep episodes and modified by novel awake experience." Proc Natl Acad Sci USA **98**(16): 9386-9390.

Hitti, F. L. and S. A. Siegelbaum (2014). "The hippocampal CA2 region is essential for social memory." Nature **508**(7494): 88-92.

Imbrosci, B., N. Nitzan, S. McKenzie, J. R. Donoso, A. Swaminathan, C. Böhm, N. Maier and D. Schmitz (2021). "Subiculum as a generator of sharp wave-ripples in the rodent hippocampus." Cell Rep **35**(3): 109021.

Ishizuka, N., J. Weber and D. G. Amaral (1990). "Organization of intrahippocampal projections originating from CA3 pyramidal cells in the rat." J Comp Neurol **295**(4): 580-623.

Jadhav, S. P., C. Kemere, P. W. German and L. M. Frank (2012). "Awake hippocampal sharp-wave ripples support spatial memory." Science **336**(6087): 1454-1458.

Joo, H. R. and L. M. Frank (2018). "The hippocampal sharp wave-ripple in memory retrieval for immediate use and consolidation." Nat Rev Neurosci **19**(12): 744-757.

Jordan, J. T. (2020). "The rodent hippocampus as a bilateral structure: A review of hemispheric lateralization." Hippocampus **30**(3): 278-292.

Jordan, J. T., M. R. Shanley and C. L. Pytte (2019). "Behavioral state-dependent lateralization of dorsal dentate gyrus c-Fos expression in mice." Neuronal Signal **3**(1): Ns20180206.

Karlsson, M. P. and L. M. Frank (2009). "Awake replay of remote experiences in the hippocampus." Nat Neurosci **12**(7): 913-918.

Kawakami, R., Y. Shinohara, Y. Kato, H. Sugiyama, R. Shigemoto and I. Ito (2003). "Asymmetrical allocation of NMDA receptor epsilon2 subunits in hippocampal circuitry." Science **300**(5621): 990-994.

Kloosterman, F., T. J. Davidson, S. N. Gomperts, S. P. Layton, G. Hale, D. P. Nguyen and M. A. Wilson (2009). "Micro-drive array for chronic in vivo recording: drive fabrication." J Vis Exp **26**: 1094.

Kohl, M. M., O. A. Shipton, R. M. Deacon, J. N. Rawlins, K. Deisseroth and O. Paulsen (2011). "Hemisphere-specific optogenetic stimulation reveals left-right asymmetry of hippocampal plasticity." Nat Neurosci **14**(11): 1413-1415.

Kravitz, A. and A. Bonci (2013). "Optogenetics, physiology, and emotions." Front Behav Neurosci **7**(169).

Langille, J. J. and R. E. Brown (2018). "The Synaptic Theory of Memory: A Historical Survey and Reconciliation of Recent Opposition." Front Syst Neurosci **12**: 52.

Lee, A. K. and M. A. Wilson (2002). "Memory of sequential experience in the hippocampus during slow wave sleep." Neuron **36**: 1183-1194.

Maguire, E. A. and C. D. Frith (2003). "Lateral asymmetry in the hippocampal response to the remoteness of autobiographical memories." J Neurosci **23**(12): 5302-5307.

Maier, N., V. Nimmrich and A. Draguhn (2003). "Cellular and Network Mechanisms Underlying Spontaneous Sharp Wave–Ripple Complexes in Mouse Hippocampal Slices."J Physiol (Lond) **550**(3): 873-887.

McHugh, T. J., K. I. Blum, J. Z. Tsien, S. Tonegawa and M. A. Wilson (1996). "Impaired hippocampal representation of space in CA1-specific NMDAR1 knockout mice." Cell **87**(7): 1339-1349.

McHugh, T. J., M. W. Jones, J. J. Quinn, N. Balthasar, R. Coppari, J. K. Elmquist, B. B. Lowell, M. S. Fanselow, M. A. Wilson and S. Tonegawa (2007). "Dentate gyrus NMDA receptors mediate rapid pattern separation in the hippocampal network." Science **317**(5834): 94-99.

McHugh, T. J. and S. Tonegawa (2009). "CA3 NMDA receptors are required for the rapid formation of a salient contextual representation." Hippocampus **19**(12): 1153-1158.

Middleton, S. J. and T. J. McHugh (2016). "Silencing CA3 disrupts temporal coding in the CA1 ensemble." Nat Neurosci **19**(7): 945-951.

Middleton, S. J. and T. J. McHugh (2019). "CA2: A Highly Connected Intrahippocampal Relay." Annu Rev Neurosci.

Morris, R. G. M., P. Garrud, J. N. P. Rawlins and J. O'Keefe (1982). "Place navigation impaired in rats with hippocampal lesions." Nature **297**: 681-683.

Nadasdy, Z., H. Hirase, A. Czurko, J. Csicsvari and G. Buzsaki (1999). "Replay and time compression of recurring spike sequences in the hippocampus." J Neurosci **19**(21): 9497-9507.

Nakashiba, T., D. L. Buhl, T. J. McHugh and S. Tonegawa (2009). "Hippocampal CA3 output is crucial for ripple-associated reactivation and consolidation of memory." Neuron **62**(6): 781-787.

Nakashiba, T., J. Z. Young, T. J. McHugh, D. L. Buhl and S. Tonegawa (2008). "Transgenic inhibition of synaptic transmission reveals role of CA3 output in hippocampal learning." Science **319**(5867): 1260-1264.

Nakazawa, K., M. C. Quirk, R. A. Chitwood, M. Watanabe, M. F. Yeckel, L. D. Sun, A. Kato, C. A. Carr, D. Johnston, M. A. Wilson and S. Tonegawa (2002). "Requirement for hippocampal CA3 NMDA receptors in associative memory recall." Science **297**(5579): 211-218.

Nakazawa, K., L. D. Sun, M. C. Quirk, L. Rondi-Reig, M. A. Wilson and S. Tonegawa (2003). "Hippocampal CA3 NMDA receptors are crucial for memory acquisition of one-time experience." Neuron **38**(2): 305-315.

O'Keefe, J. (1976). "Place units in the hippocampus of the freely moving rat." Exp Neurol **51**(1): 78-109.

O'Keefe, J. and J. Dostrovsky (1971). "The hippocampus as a spatial map: preliminary evidence from unit activity in the freely-moving rat." Brain Res. **34**: 171-175.

O'Keefe, J. and L. Nadel (1978). The Hippocampus as a Cognitive Map. Oxford, Clarendon Press.

O'Keefe, J. and M. L. Recce (1993). "Phase relationship between hippocampal place units and the EEG theta rhythm." Hippocampus **3**: 317-330.

Ólafsdóttir, H. F., D. Bush and C. Barry (2018). "The Role of Hippocampal Replay in Memory and Planning." Curr Biol **28**(1): R37-r50.

Oliva, A., A. Fernandez-Ruiz, G. Buzsaki and A. Berenyi (2016). "Role of Hippocampal CA2 Region in Triggering Sharp-Wave Ripples." Neuron **91**(6): 1342-1355.

Oliva, A., A. Fernandez-Ruiz, F. Leroy and S. A. Siegelbaum (2020). "Hippocampal CA2 sharp-wave ripples reactivate and promote social memory." Nature **587**(7833): 264-269.

Omer, D. B., S. R. Maimon, L. Las and N. Ulanovsky (2018). "Social place-cells in the bat hippocampus." Science **359**(6372): 218-224.

Peyrache, A., K. Benchenane, M. Khamassi, S. I. Wiener and F. P. Battaglia (2010). "Principal component analysis of ensemble recordings reveals cell assemblies at high temporal resolution." J Comput Neurosci **29**(1-2): 309-325.

Pfeiffer, B. E. and D. J. Foster (2013). "Hippocampal place-cell sequences depict future paths to remembered goals." Nature **497**(7447): 74-79.

Pfeiffer, B. E. and D. J. Foster (2015). "PLACE CELLS. Autoassociative dynamics in the generation of sequences of hippocampal place cells." Science **349**(6244): 180-183.

Rothschild, G., E. Eban and L. M. Frank (2017). "A cortical-hippocampal-cortical loop of information processing during memory consolidation." Nat Neurosci **20**(2): 251-259.

Roux, L., B. Hu, R. Eichler, E. Stark and G. Buzsáki (2017). "Sharp wave ripples during learning stabilize the hippocampal spatial map." Nat Neurosci **20**(6): 845-853.

Scarf, D., J. Gross, M. Colombo and H. Hayne (2013). "To have and to hold: episodic memory in 3- and 4-year-old children." Dev Psychobiol **55**(2): 125-132.

Schiavo, G., F. Benfenati, B. Poulain, O. Rossetto, P. Polverino de Laureto, B. R. DasGupta and C. Montecucco (1992). "Tetanus and botulinum-B neurotoxins block neurotransmitter release by proteolytic cleavage of synaptobrevin." Nature **359**(6398): 832-835.

Schiller, D., H. Eichenbaum, E. A. Buffalo, L. Davachi, D. J. Foster, S. Leutgeb and C. Ranganath (2015). "Memory and Space: Towards an Understanding of the Cognitive Map." J Neurosci **35**(41): 13904-13911.

Schmitzer-Torbert, N., J. Jackson, D. Henze, K. Harris and A. D. Redish (2005). "Quantitative measures of cluster quality for use in extracellular recordings." Neuroscience **131**(1): 1-11.

Schoch, S., F. Deák, A. Königstorfer, M. Mozhayeva, Y. Sara, T. C. Südhof and E. T. Kavalali (2001). "SNARE function analyzed in synaptobrevin/VAMP knockout mice." Science **294**(5544): 1117-1122.

Scoville, W. B. and B. Milner (1957). "Loss of recent memory after bilateral hippocampal lesions." J Neuropsychiatry Clin Neurosci **12**(1): 103-113.

Shansky, R. M. (2019). "Are hormones a "female problem" for animal research?" Science **364**(6443): 825-826.

Sharp, P. E., H. T. Blair, D. Etkin and D. B. Tzanetos (1995). "Influences of vestibular and visual motion information on the spatial firing patterns of hippocampal place cells." J Neurosci **15**(1 Pt 1): 173-189.

Shinohara, Y., H. Hirase, M. Watanabe, M. Itakura, M. Takahashi and R. Shigemoto (2008). "Left-right asymmetry of the hippocampal synapses with differential subunit allocation of glutamate receptors." Proc Natl Acad Sci USA **105**(49): 19498-19503.

Shinohara, Y., A. Hosoya and H. Hirase (2013). "Experience enhances gamma oscillations and interhemispheric asymmetry in the hippocampus." Nat Commun **4**: 1652.

Shinohara, Y., A. Hosoya, K. Yahagi, A. S. Ferecsko, K. Yaguchi, A. Sik, M. Itakura, M. Takahashi and H. Hirase (2012). "Hippocampal CA3 and CA2 have distinct bilateral innervation patterns to CA1 in rodents." Eur J Neurosci **35**(5): 702-710.

Shinohara, Y., A. Hosoya, N. Yamasaki, H. Ahmed, S. Hattori, M. Eguchi, S. Yamaguchi, T. Miyakawa, H. Hirase and R. Shigemoto (2012). "Right-hemispheric dominance of spatial memory in split-brain mice." Hippocampus **22**(2): 117-121.

Shipton, O. A., M. El-Gaby, J. Apergis-Schoute, K. Deisseroth, D. M. Bannerman, O. Paulsen and M. M. Kohl (2014). "Left-right dissociation of hippocampal memory processes in mice." Proc Natl Acad Sci USA **111**(42): 15238-15243.

Silva, D., T. Feng and D. J. Foster (2015). "Trajectory events across hippocampal place cells require previous experience." Nat Neurosci **18**(12): 1772-1779.

Skaggs, W. E. and B. L. McNaughton (1996). "Replay of neuronal firing sequences in rat hippocampus during sleep following spatial experience." Science **271**(5257): 1870-1873.

Skaggs, W. E. and B. L. McNaughton (1996). "Replay of neuronal firing sequences in rat hippocampus during sleep following spatial experience." Science **271**(1870-1873).

Skaggs, W. E., B. L. McNaughton and K. M. Gothard (1993). An Information-Theoretic Approach to Deciphering the Hippocampal Code. Advances in Neural Information Processing Systems, Morgan Kaufmann Publishers Inc.

Skaggs, W. E., B. L. McNaughton, M. A. Wilson and C. A. Barnes (1996). "Theta phase precession in hippocampal neuronal populations and the compression of temporal sequences." Hippocampus **6**(2): 149-172.

Song, D., D. Wang, Q. Yang, T. Yan, Z. Wang, Y. Yan, J. Zhao, Z. Xie, Y. Liu, Z. Ke, T. J. Qazi, Y. Li, Y. Wu, Q. Shi, Y. Lang, H. Zhang, T. Huang, C. Wang, Z. Quan and H. Qing (2020). "The lateralization of left hippocampal CA3 during the retrieval of spatial working memory." Nat Commun **11**(1): 2901.

Steinvorth, S., B. Levine and S. Corkin (2005). "Medial temporal lobe structures are needed to re-experience remote autobiographical memories: evidence from H.M. and W.R." Neuropsychologia **43**(4): 479-496.

Sullivan, D., J. Csicsvari, K. Mizuseki, S. Montgomery, K. Diba and G. Buzsaki (2011). "Relationships between hippocampal sharp waves, ripples, and fast gamma oscillation: influence of dentate and entorhinal cortical activity." J Neurosci **31**(23): 8605-8616.

Suzuki, S. S. and G. K. Smith (1987). "Spontaneous EEG spikes in the normal hippocampus. I. Behavioral correlates, laminar profiles and bilateral synchrony." Electroencephalogr Clin Neurophysiol **67**(4): 348-359.

Szirmai, I., G. Buzsáki and A. Kamondi (2012). "120 years of hippocampal Schaffer collaterals." Hippocampus **22**(7): 1508-1516.

Tang, W. and S. P. Jadhav (2019). "Sharp-wave ripples as a signature of hippocampal-prefrontal reactivation for memory during sleep and waking states." Neurobiol Learn Mem **160**: 11-20.

Thompson, L. T. and P. J. Best (1990). "Long-term stability of the place-field activity of single units recorded from the dorsal hippocampus of freely behaving rats." Brain Res **509**(2): 299-308.

Tsien, J. Z., P. T. Huerta and S. Tonegawa (1996). "The essential role of hippocampal CA1 NMDA receptor-dependent synaptic plasticity in spatial memory." Cell **87**: 1327-1338.

Tulving, E. (1983). Elements of Episodic Memory. Oxford, Clarendon Press.

Tulving, E. (2002). "Episodic memory: from mind to brain." Annu Rev Psychol **53**: 1-25.

van de Ven, G. M., S. Trouche, C. G. McNamara, K. Allen and D. Dupret (2016). "Hippocampal Offline Reactivation Consolidates Recently Formed Cell Assembly Patterns during Sharp Wave-Ripples." Neuron **92**(5): 968-974.

Vanderwolf, C. H. (1969). "Hippocampal electrical activity and voluntary movement in the rat." Electroencephalogr Clin Neurophysiol **26**(4): 407-418.

Villalobos, C., P. E. Maldonado and J. L. Valdés (2017). "Asynchronous ripple oscillations between left and right hippocampi during slow-wave sleep." PLoS One **12**(2): e0171304.

Wilson, M. A. and B. L. McNaughton (1993). "Dynamics of the hippocampal ensemble code for space." Science **261**: 1055-1058.

Wilson, M. A. and B. L. McNaughton (1994). "Reactivation of hippocampal ensemble memories during sleep." Science **265**(5172): 676-679.

Witter, M. P. (2007). "Intrinsic and extrinsic wiring of CA3: indications for connectional heterogeneity." Learn Mem **14**(11): 705-713.

Yamamoto, J. and S. Tonegawa (2017). "Direct Medial Entorhinal Cortex Input to Hippocampal CA1 Is Crucial for Extended Quiet Awake Replay." Neuron **96**(1): 217-227.

Zielinski, M. C., W. Tang and S. P. Jadhav (2020). "The role of replay and theta sequences in mediating hippocampal-prefrontal interactions for memory and cognition." Hippocampus **30**(1): 60-72.

Ziv, Y., L. D. Burns, E. D. Cocker, E. O. Hamel, K. K. Ghosh, L. J. Kitch, A. E. Gamal and M. J. Schnitzer (2013). "Long-term dynamics of CA1 hippocampal place codes." Nat Neurosci **16**: 264-267.

List of research achievements for application of Doctor of Science, Waseda University

Full Name 関　鶴菲　　seal or signature

Date Submitted(yyyy/mm/dd): 2021/10/30

種類別 (By Type)	題名、 発表・発行掲載誌名、 発表・発行年月、 連名者（申請者含む） (theme, journal name, date & year of publication, name of authors inc. yourself)
Paper	○Hefei Guan, Steven J. Middleton, Takafumi Inoue, Thomas J. McHugh,"Lateralization of CA1 assemblies in the absence of CA3 input", Nature Commnunications, 12:6114 (2021)
Poster	Hefei Guan, Arthur J.Y. Huang, Denis Polygalov, Takafumi Inoue, Thomas J. McHugh (2017). The impact of transient silencing of the retrosplenial cortex on hippocampal physiology. Society for Neuroscience Annual Meeting, November 2017.